THERMOELECTRIC BEHAVIOR OF FLEXIBLE ORGANIC NANOCOMPOSITES WITH CARBON NANOTUBES

A Dissertation

by

KYUNG WHO CHOI

Submitted to the Office of Graduate and Professional Studies of
Texas A&M University
in partial fulfillment of the requirements for the degree of

DOCTOR OF PHILOSHOPHY

Chair of Committee,	Choongho Yu
Committee Members,	Devesh Ranjan
	Sy-Bor Wen
	Jodie Lutkenhaus
Head of Department,	Andreas A. Polycarpou

December 2013

Major Subject: Mechanical Engineering

ABSTRACT

There have been significant researches about thermoelectric behaviors by applying carbon nanotube (CNT)/polymer nanocomposites. Due to its thermally disconnected but electrically connected junctions between CNTs, the thermoelectric properties were dramatically increased. Functionalized CNTs with metal nano particles or organic molecules can manipulate the intrinsic properties of nanocomposties to p- or n-type semiconductors by electron depletion or injection. In order to have low thermal conductivity composite, low concentration of CNT was required to form a non-percolated network in the composite, so as to manipulate the thermoelectric properties of conductive polymer matrix. According to above series of studies, ~10mV/K of thermopower was achieved with ~100 S/m of electrical conductivity, resulting ~10,000 $\mu W/m\text{-}K^2$ of power factor. The result of this study shows that organic thermoelectric materials would be a promising approach for thermoelectric applications with light-weight and non-toxic nature.

DEDICATION

This dissertation is dedicated to my brilliant and beloved and supportive wife, Songyi Kim, our sweet and kind-hearted little girls, Claire and Olivia Choi, and to my always encouraging, ever faithful parents, Mooho Choi and Younghee Kim.

ACKNOWLEDGEMENTS

I appreciate the efforts and support of Dr. Choongho Yu for his guidance with research and this thesis, both of which would not have been accomplished without his input. I would like to thank my committee members Dr. Ranjan, Dr. Wen, and Dr. Lutkenhaus for their guidance and knowledge which contributed to this research. I am also indebted to several people who helped me with the experimental portions of this work, especially in our group, Nano Energy lab members.

Finally, I would like to thank to my whole family for their love and support, and for encouraging me to pursue my degree.

TABLE OF CONTENTS

Page

Page

LIST OF FIGURES

Page

Page

Page

LIST OF TABLES

Page

CHAPTER I

INTRODUCTION AND LITERATURE REVIEW

1.1 Introduction

Thermoelectric devices are efficient for regenerating the waste heat from our daily life energy generation systems, such as conventional heat engines or power plant. From the theory by Seebeck and Thomson, the thermoelectric systems can get electricity from the temperature gradient, and heat up or cool down a system by voltage difference. This is because the electron carriers move away from a cold side to hot side, hence the current can be passed from n-type leg to the p-type leg. There is usually a large temperature difference in general heat engines. This temperature gradient is inevitable because there should be a high temperature source and a low temperature sink to convert heat to useful work. From the 2nd law of thermodynamics, there should be a heat rejection to low temperature sink which makes the efficiency of the system below 100%. The advantage of the thermoelectric system is recovering this useless, but has to be discarded energy by applying it into the pre-existing two different temperature sources. Furthermore, the thermoelectric system can be a good candidate for special application such as super silence cooling or heating. This is possible due the simple structure without any moving part in it. This strong point also makes this system to be applied as a power generator or tiny cooler in micro electric mechanical systems (MEMS). There has

been almost no improvement in the efficiency of thermoelectric materials in the past 40 years [1], although such kinds of attractable aspects. It has been known that Bi-Te based alloy shows the best performance in thermoelectric manner [2-4], but there are some weaknesses which impede wide thermoelectric applications. For example, Te is one of the rarest elements on earth, and this makes it expensive. Furthermore, the toxicity of Te prevents it from being applied to general purpose. The difficult manufacturing process of Bi-Te based semiconducting materials is also one of the shortages. Such kinds of disadvantages can be compensated with polymer based thermoelectric materials.

1.2 Literature review

1.2.1 *Selective transport mechanism*

The performance of thermoelectric is defined as a figure of merit. This is expressed in $ZT = S^2\sigma T / k$, where S and σ are Seebeck coefficient and electrical conductivity, respectively, ZT the thermoelectric figure of merit, T the environment temperature, and k is thermal conductivity of the material. According to above equation, low thermal conductivity of polymeric materials is promising for thermoelectric applications [5, 6], but their low electrical conductivities and Seebeck coefficients (thermopowers) have excluded them as a feasible candidate in the past. Here, nanomaterial-polymer composites bring their electrical properties into degenerate-semiconductor or metallic regimes by incorporating conductive fillers into a polymer matrix. The nanocomposite samples were prepared by mixing the emulsion type of poly (vinyl acetate) and carbon nanotubes (CNT) together. Then the solution was dried to

make the network structure of polymer and CNTs. These polymer composites are adequate for thermoelectric material because the junctions between CNTs act like a high way for electrons, but a barrier for phonons. In this type of polymer composite, the stabilizers have important role for energy transport between junctions. The effects of stabilizers were revealed by replacing the different types of stabilizers and altering mixed amount. The influence of CNT concentration and proper ratio of CNT and stabilizer on thermoelectric properties also studied to figure out the maximum electrical properties. The electrical conductivity of the composites was increased over 10^5 S/m with a thermopower of typical carbon nanotubes and a thermal conductivity of typical polymers. The results show polymers can be viable for thermoelectric energy conversion, replacing heavy and toxic materials such as Bi-Te alloys in the future.

1.2.2 *Effect of stabilizers in nanocomposites*

In typical bulk semiconductors, thermoelectric properties are strongly correlated, making ZT enhancement very difficult. For example, an increase of electrical conductivity often accompanies a decrease of thermopower and an increase of thermal conductivity. Despite these trends in typical solids, previous study with CNTs and poly(vinyl acetate)(PVAc) latex showed that it is possible to increase electrical conductivity and keep thermopower and thermal conductivity relatively constant [7]. This behavior is governed by electrically connected but thermally disconnected junctions between CNTs. A small energy barrier for electron transport at the junctions plays an important role in deterring low energy electron transport, making thermopower

insensitive to the increase of electrical conductivity. The barrier for energy carrier transport across the junctions can be significantly altered by changing stabilizers that are necessary for dispersing and exfoliating CNTs [8, 9] which naturally form bundles due to van der Waals force between them. Highly entangled nanotubes are difficult to disperse in organic solvent or water without a stabilizer, resulting in disconnected or less-branched networks. Electron transport across junctions is influenced by interparticle distance, electronic states of CNTs, contact potential barriers, and electrostatic charges of CNTs and matrices [10, 11], which can be altered with stabilizing agents. There are several types of stabilizers that have been used to disperse nanotubes in polymers such as surfactants [12-15], polymers [16-19], biomolecules [20, 21], and inorganic nanoparticles [22, 23]. Most dispersants are electrical insulators that hinder electron transport across the junctions. Recently, it was shown that an intrinsically conductive polymer, poly(3,4-ethylenedioxythiophene): poly(styrene sulfonate) (PEDOT:PSS), can effectively stabilize and disperse nanotubes in water [11], thereby enhancing electrical conductivity by preventing settling and aggregation of CNTs. PEDOT:PSS has been widely used as an antistatic coating material, electrodes for capacitors or photodiodes, transparent electrodes for solar cells, and a hole transport layer for organic LED [18, 24-27]. Its electrical conductivity can be greatly enhanced with solvent doping such as dimethyl sulfoxide (DMSO) [24].

1.2.3 *Organic films with large thermoelectric power*

The organic material modifies the junctions between nanotubes, suppressing phonon transport but maintaining electronic properties. In order to increase electrical conductivity, carbon nanotubes were added to the organic materials because their "intrinsic" electrical conductivities were reported to be very high up to ~2×10^7 S/m at room temperature [28]. Nevertheless, nanotubes have been considered to be irrelevant for thermoelectric applications due to high intrinsic thermal conductivity, ~10^3 W/m-K at room temperature [29, 30]. The thermal conductivity, however, can be considerably reduced when nanotubes are bundled in bulk-scale materials. For instance, the thermal conductivities of nanotube mats [31] and beds [32] were measured to be ~210 and 0.1~0.2 W/m-K at 300 K, respectively. In nanocomposites, thermal conduction through nanotubes was substantially impeded by sandwiching organic particles between the nanotubes whose vibrational spectra are different from those of the particles. Such mismatches often effectively block phonon transport and thereby suppress thermal conductivity. Despite the large barrier for phonons, electrons can be transported across the junction since PEDOT:PSS has relatively high electrical conductivity up to ~10^4 S/m [33].

1.2.4 *Functionalized CNTs with metal nanoparticles*

Carbon nanotubes (CNTs) have been considered as promising candidates for various applications including field effect transistors (FETs) [34, 35], touch screens [36, 37], field emission displays (FEDs) [38, 39], and solar cells [40-42] due to their

outstanding electrical properties. Recently, CNTs were used as fillers in polymer composites and their electrical conductivities were orders of magnitude higher than other polymer composites with conductive fillers [7, 43-46]. It has been shown that the electrical conductivity can be dramatically increased as a function of nanotube loadings in the composites. The highest electrical conductivity was obtained with 60 wt%, but the conductivity was decreased with composites containing CNTs more than 60 wt% [46]. The reduction in electrical conductivity is due to CNT aggregations caused by the insufficient amount of dispersants (which cannot be increased due to high CNT loadings). The optimum ratio of CNT to stabilizer for high electrical conductivity was found to be 3:2. This means that the maximum CNT concentration should not be larger than 60 wt% for improving conductivity.

Nanoparticles can be precipitated on nanotubes by galvanic displacement or reduction potential differences between nanotubes and nanoparticles [47]. When nanoparticles are precipitated on nanotubes, charge transfer between them occurs, altering electrical transport properties of the nanotubes. Such property changes are similar to semiconductor doping with an acceptor impurity.

1.2.5 *n-type doping on CNTs with organic molecules*

Several methods have been demonstrated for the production of air stable n-type nanotubes, including passivation of a protective film around the tubes to prevent oxygen doping, application of viologens for a direct redox reactions, and the use of metal electrodes with low work functions [48-50]. A simpler production method has also been

demonstrated wherein the physical adsorption of branched polyethylene imine (PEI) onto carbon nanotubes results in a conversion of the conducting properties from p-type back to n-type [51, 52]. Nanotubes functionalized with PEI have been used to produce p-n junctions, photovoltaic cells, and field-effect transistors [51, 53-55]. In previous work, the thermopower of thin films composed of PEI-doped tubes was measured to be as large as -60 μV/K [52]. Such films, composed almost purely of carbon nanotubes, are not prime candidates for thermoelectric generation because their thermal energy transport is too high due to their intrinsically high thermal conductivity [29].

1.2.6 *Thermoelectric efficiency in devices*

As shown above chapter (1.2.1), the efficiency of generated thermoelectric voltage in a material was determined by its figure of merit, *ZT*. Of course, the *ZT* depends on the material properties such as electrical conductivity, thermopower, and thermal conductivity. However, it is not reasonable to define the efficiency of a thermoelectric device by *ZT* since the actual power generation is proportional to the current flow in the circuit as well as the operation temperature which would be related to the hot and cold side of the device. Hence, the thermal efficiency was given when the external load and device resistance is equivalent [56];

$$\eta_{\max} = \frac{T_h - T_c}{T_h} \frac{\sqrt{1+ZT_m} - 1}{\sqrt{1+ZT_m} + T_c / T_h} \quad (1)$$

where T_m is the average temperature or operation temperature, T_h the hot side temperature, T_c the heat sink temperature. As can be seen, the maximum efficiency is limited by the Carnot efficiency ($(T_h - T_c)/T_h$), like all heat engines.

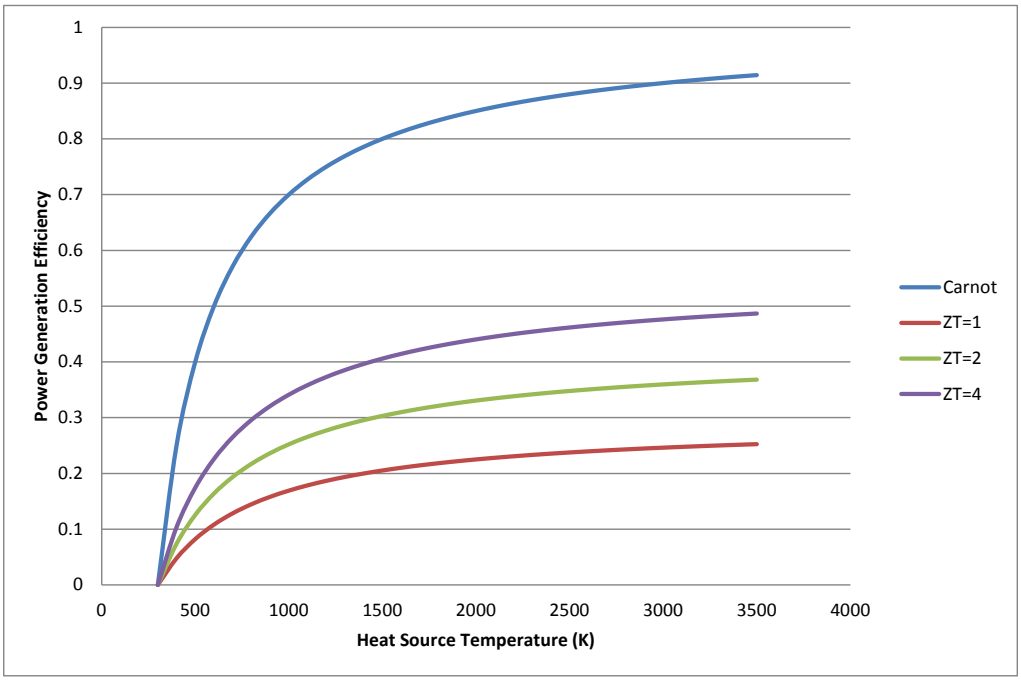

Figure 1. Power generation efficiency versus temperature of the hot side. The cold side is fixed as room temperature.

In the above equation, some assumptions were applied such as no contact resistance and constant *ZT* values through all the temperature range. From Figure 1, it is possible to reach 30% of thermal efficiency with *ZT* of 2 when the temperature of hot side is 1300K and that of cold side is assumed as room temperature. However, to achieve 30% of efficiency, p- and n-type materials are required, and the average *ZT* of 2 for both of materials is needed near 1300K, not a peak value of 2. For large temperature gradient, segmentation of different materials which have peak *ZT* at different temperatures will

improve device *ZT* [57]. In this case, the electrical current required for highest efficiency operation changes as the thermoelectric properties of the material will be varied with temperature. Hence, the thermoelectric compatibility factors should be similar.

Thermoelectric device testing is challenging since measurement of heat transfer to the hot side and that from cold side is not easy. There are unknown thermal leakages from the electrodes and thermocouples, and radiation loss is not negligible as well. Therefore, further research is required for thermoelectric device testing such as solving the problems in contact barriers or thermal expansion coefficient of the materials at large temperature gradients.

1.2.7 *Electronic structure of organic conductors*

The conductive polymers can be "conductive" since the electronic properties are based on sp2 hybridized linear carbon chains. Four valence electrons in 2s and 2p take part in chemical bonds. Different from sp3 hybridized covalent bond in insulating polymers, pi-electrons can be delocalized along the chain, and travel through conjugated pz orbital like free electrons in metals. Highly electrically conductive properties in carbon nanotubes also based on the same mechanism.

In organic conductors, certain energy levels are represent conduction or valence band in inorganic materials, which are HOMO (highest occupied molecular orbital) and LUMO (lowest unoccupied molecular orbital), respectively. In order to inject electron or hole to the organic material, LUMO and HOMO levels where electrons and holes can be travel are required to be aligned. Different from independent molecules, when the

electron or hole is injected into molecular solid, the environment electrons are stabilized by polarization. The polarization in molecular level will effect on atomic bonds, and finally distorts the molecular structures. This distortion will follow the electron or hole when they are moving through the molecules to induce a current flow (polaron).

The properties of metals, semiconductors, and insulators can be most easily described using simple, non-polymeric solids as an example. In metals, the electrons which are close to the top of the filled orbitals in continuous orbitals can easily jump to unoccupied levels without any energy. In order to explain the mechanism, electron distribution in a certain temperature is usually used. Here, the Fermi level is defined as the highest occupied energy level at T=0. If the temperature is larger than 0, it would be hard to distinguish occupied and unoccupied levels, because the thermal energy will induce electron hopping. Of course, more and more electrons can be excited from unoccupied level to occupied level when the temperature is increased. The Fermi-Dirac distribution can describe this population of orbitals at different temperatures. The mean value in the Fermi-Dirac distribution is the Fermi energy, which is assigned to the energy level that is half occupied. Therefore, it can be said that the Fermi energy is a function of temperature. The electrical conductivity in metal will be changed by environment temperature. For example, the conductivity will be decrease with elevated temperature even though much more electrons are excited. This is because electron-electron or electron-atom scattering will be occurred due to too much thermal motion of the atoms, resulting less effective electron transport through the material. Different from metals, there is an energy band gap between conduction and valence band in

semiconductors and insulators. If the temperature is increased, the electrons in valence band can be excited and fill the conduction band by enough thermal energy. Then the electrons can be mobile and the material becomes electrically conductive. In insulators, the energy gap is too large to be overcome. Hence most of electrons in valence band cannot be excited to conduction band, and the overall conductivity will be closed to zero.

CHAPTER II

IMPROVED THERMOELECTRIC BEHAVIOR OF ORGANIC NANOCOMPOSITES WITH CONDUCTIVE STABILIZER*

2.1 Introduction

The thermoelectric properties of carbon nanotube (CNT)-filled polymer composites can be enhanced by modifying junctions between CNTs using poly(3,4-ethylenedioxythiophene) poly(styrenesulfonate)(PEDOT:PSS), yielding high electrical conductivities (up to ~40000 S/m) without significantly altering thermopower (or Seebeck coefficient). This is because PEDOT:PSS particles are decorated on the surface of CNTs, electrically connecting junctions between CNTs. On the other hand, thermal transport remains comparable to typical polymeric materials due to the dissimilar bonding and vibrational spectra between CNT and PEDOT:PSS. This behavior is very different from that of typical semiconductors whose thermoelectric properties are strongly correlated. The decoupled thermoelectric properties, which is ideal for developing better thermoelectric materials, are believed to be due to thermally disconnected and electrically connected contact junctions between CNTs. Carrier transport at the junction is found to be strongly dependent on the type and concentration of stabilizers. The crucial role of stabilizers was revealed by characterizing transport

* Parts of this section are reprinted from "Improved thermoelectric behavior of nanotube-filled polymer composites with Poly(3,4-ethylenedioxythiophene) Poly(styrenesulfonate)," by D. Kim, Y. Kim, K. Choi, J. C. Grunlan, and C. Yu, ACS Nano, 4, 513-523 (2010) with permission by ACS Nano.

characteristics of composites synthesized by electrically conducting PEDOT:PSS and insulating gum Arabic (GA) with 1:1 ~ 1:4 weight ratios of CNT to stabilizers. The influence of composite synthesis temperature and CNT-type and concentration on thermoelectric properties has also been studied. Single-walled (SW) CNT-filled composites dried at room temperature followed by 80 °C exhibited the best thermoelectric performance in this study. The highest thermoelectric figure of merit (*ZT*) in this study is estimated to be ~0.02 at room temperature, which is at least one order of magnitude higher than most polymers and higher than that of bulk Si. Further studies with various polymers and nanoparticles with high thermoelectric performance may result in economical, lightweight, and efficient polymer thermoelectric materials.

2.2 Experimental

A vinyl acetate_ethylene copolymer emulsion (Airflex 401 made by Air Products, Inc.) served as a matrix material of the composite for this study. This latex contains 55.2 wt % solids in water and exhibits a T_g of -15 °C when dried into a film. Prior to drying, the Airflex emulsion exists as an aqueous suspension of polydispersed polymer particles that are 0.14 ~ 3.5 μm in diameter (an average diameter of ~650 nm). XM-grade CNTs (XM-CNTs) and purified single-wall carbon nanotubes (SWCNTs) were purchased from Carbon Nanotechnologies. XM-CNTs are a mixture of metallic and semiconducting single-, double-, and triple-walled CNTs. Gum arabic (GA) purchased from Sigma- Aldrich was used as a stabilizer for the nanotubes in water. The other stabilizer, poly(3,4-ethylenedioxythiophene) doped with poly(styrenesulfonate)

(PEDOT:PSS), was purchased from H. C. Starck. PEDOT:PSS exists as a suspension containing 1.3 wt % solids (0.5 wt % PEDOT and 0.8 wt % PSS) in water.

To increase electrical conductivity, PEDOT: PSS was mixed with DMSO (Sigma-Aldrich, Co.) for 2 h at room temperature. Next, CNTs were combined with either the PEDOT:PSS suspension or 2 wt % GA in water by sonication with a VirTis Virsonic 100 ultrasonic cell disrupter (SP industries, Inc.) for ~15 min at ~50 W. The Airflex emulsion and deionized water were then added to the CNT/stabilizer mixtures to obtain an aqueous precomposite mixture of 2.5 wt % total solids (except for the composites with 20 and 35 wt % CNT concentrations, whose total solids were_1.5 wt % or less to reduce viscosity) followed by several minute sonication. Total solid weight including water is typically 20 g. The pH value of the composite mixtures were then adjusted to 2~2.9 because carbon nanotubes are well dispersed at this pH level. All sample concentrations are based upon the total dry weight of the composite, which includes CNTs, emulsion solids, GA, and PEDOT:PSS. Solid composites were made by drying aqueous mixtures in a 26 cm^2 plastic mold for ~5 days under ambient conditions and then for 24 h in a vacuum desiccator prior to testing to completely remove residual water. The thicknesses of the tested composites were 0.07~0.13 mm.

Electrical conductivity and thermopower were measured with a homemade shielded four point probe apparatus with a Keithley 2000 Multimeter (Cleveland, OH) and a GW PPS-3635 power supply (Good Will Instrument Co., LTD) in conjunction with Labview (National Instruments, Austin, TX). Composite microstructures were imaged with an FEI Quanta 600 field-emission scanning electron microscope (Hillsboro,

OR). Films were soaked in liquid nitrogen and fractured by hand and the surfaces were sputter-coated with 4 nm of platinum prior to SEM imaging. For electrical conductivity and thermopower measurements, samples were cut into pieces of a rectangular shape (typically ca. 30 mm × 7 mm) and suspended by using a thermal paste between two thermoelectric devices (typically ~15 mm apart) used for creating temperature difference. Electrical conductance was measured by using a current-voltage (*I*-*V*) sweeping measurement technique with four-point probes after four metal lines were patterned with a silver paint. For the thermopower measurement, temperature gradients along the long edge of the sample were measured by two T-type thermocouples. The thermoelectric voltages were measured while the temperature gradient was altered. Thermal conductivity was measured along the film thickness direction with a homemade ASTM D5470 standard setup.

2.3 Results and discussion

The thermoelectric properties of CNT-filled polymer composites were studied with different types of surfactants and varying their ratio to CNT in the composites. Different from insulating gum Arabic (GA), poly(3,4-ethylenedioxithiophene) poly(styrenesulfonate)(PEDOT:PSS), which is one of the representative conductive polymer, incorporated composites show high electrical conductivity since PEDOT:PSS particles are coated on the surface of the CNTs and enhancing the tube-tube junctions electrically conductive.

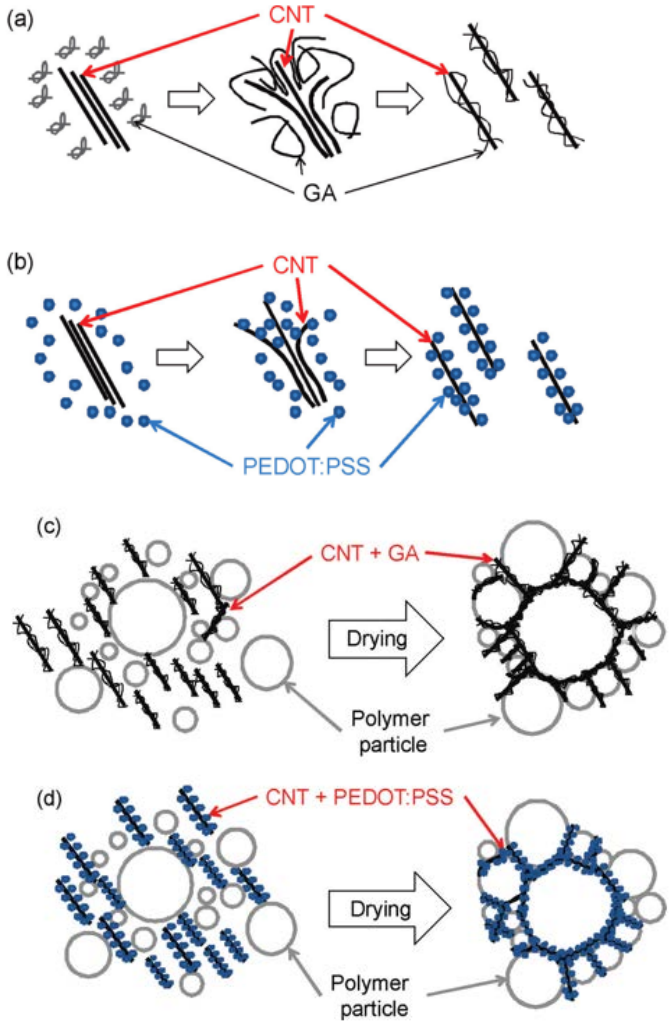

Figure 2. CNTs form a three-dimensional network along the surface of spherical emulsion particles. (a) and (b) show how CNTs were dispersed by GA and PEDOT:PSS, respectively. (c) and (d) illustrate segregated network formation before (left) and after (right) the drying of water-based polymer emulsions (reprinted from [45]).

In order to synthesize the composites, the nanotubes and stabilizers were mixed and made into aqueous solution with vigorous sonication. After this, the nanotubes and polymer particles are uniformly dispersed in DI water, and the polymer emulsions push the nanotubes into interstitial spaces to form a segregated network while water is

evaporated. Figure 2 panels (a) and (b) show schematics of CNTs dispersed by GA and PEDOT:PSS. Both dispersants exfoliate CNTs and modify their surfaces, making CNTs hydrophilic and thereby stabilized in water. Figure 2 panels (c) and (d) illustrate the formation of a segregated network during the drying of water-based polymer emulsions that occurs after addition of stabilized CNTs. Initially, the nanotubes and polymer particles are uniformly dispersed in water (left). During drying (water evaporation), the polymer particles push the nanotubes into interstitial spaces to form a segregated network (right). The composite matrix is a copolymer latex containing vinyl acetate and ethylene. Because of the low glass transition temperature (T_g) of this polymer emulsion (-15 °C), it is more flexible than the poly(vinyl acetate) homopolymer (T_g = 35 °C) that was used to make composites reported earlier [7]. XM CNTs (Carbon Nanotechnologies, Inc.), which are a mixture of metallic and semiconducting single-, double-, and triple-walled CNTs, were used as a low cost alternative to SWCNTs. Higher quality SWCNTs were also used to achieve enhanced thermoelectric performance with the best recipe for XM-CNT filled composites.

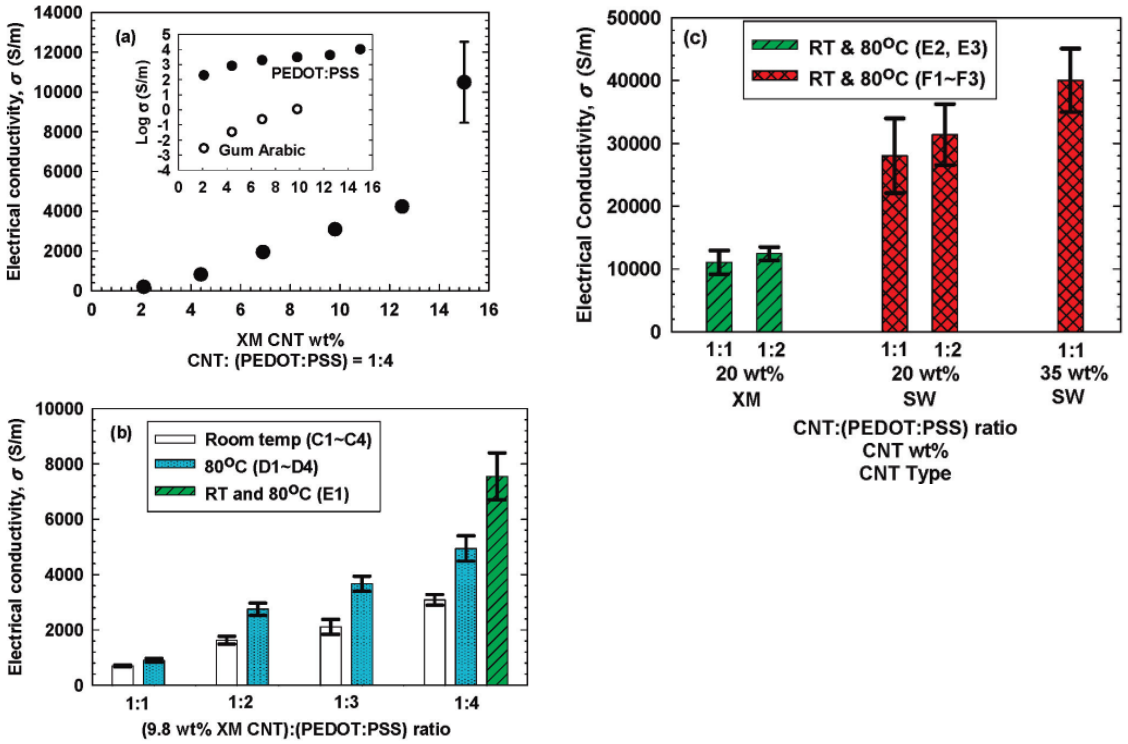

Figure 3. (a) Electrical conductivities of 2.1, 4.4, 6.9, 9.8, 12.5, or 15 wt% CNT composites at room temperature. To compare the role of the stabilizer, electrical conductivity of samples with GA (hollow circles) is plotted in the linear-log scale inset with those with PEDOT:PSS. (b) Electrical conductivities of the composites with 1:1, 1:2, 1:3, or 1:4 ratio between CNT and PEDOT:PSS. CNT concentration is fixed to 9.8 wt%. (c) Electrical conductivities of the composites with CNT (20 wt%) or SWCNT (20 or 35 wt%) and 1:1 or 1:2 ration between CNT and PEDOT:PSS at room temperature (reprinted from [45]).

As the CNT concentration increases, the electrical conductivity is dramatically enhanced. A conductivity of ~11700 S/m was obtained at 15 wt% of CNT concentration (CNT:(PEDOT:PSS) = 1:4) is comparable to that of the composite prepared with 20 wt% CNT loading and 1:2 ratio of CNT to PEDOT:PSS. Note that electrical conductivities of 10^{-2} ~10^{1} S/m are typically observed in traditional nanotube-filled polymer composites with similar concentrations [10, 58, 59]. On the other hand, when

the composites were stabilized with GA, electrical conductivity was lowered by a factor of 10^4 or more, as indicated in Figure 3(a). This is a strong indication that electronic properties can be manipulated by altering junctions between nanoparticles. For better thermoelectric energy conversion, it is necessary to pass as many electrons as possible across the junctions for high electrical conductivity, while low energy electron transport is deterred at the junctions for large thermopower.

To study the role of PEDOT:PSS, the concentration of PEDOT:PSS was varied with fixed CNT concentrations (9.8 and 20 wt %). Furthermore, the influence of the drying condition and filler type on transport properties was investigated. Figure 3(b) shows the electrical conductivities of composites with 1:1, 1:2, 1:3, or 1:4 weight ratio of 9.8 wt % XM-CNTs to PEDOT:PSS. These composites were dried at room temperature, 80 °C, or combination of room temperature and 80 °C, as described earlier. As the PEDOT:PSS ratio is increased, electrical conductivity is consistently enhanced irrespective of the drying condition. PEDOT:PSS is electrically conductive, resulting in electrically less resistive tube - tube junctions and self-made electron pathways. Increasing the PEDOT:PSS loading results in a large number of electrically bridged junctions until the conductivity becomes similar to that of completely covered tubes. The electrical conductivity of the sample dried at 80 °C was increased as much as 1.5~2 times compared to the sample dried at room temperature because this elevated temperature often tightens nanoparticle networks. In addition, the composites dried at room temperature show a significant level of porosity due to intertube gaps. These pores can be eliminated when the drying temperature is raised to 80 °C because the emulsion

particles effectively deform around CNTs and fill the gaps between them. The enhancement in electrical conductivity from the mixed drying condition comes from a slow drying process (*e.g.*, more time for segregation) during the initial stage of the segregated network formation. Additionally, 20 wt % CNT dispersed by 40 wt % PEDOT:PSS (total electrically conductive solids are 60 wt %) was synthesized with the mixed drying condition. Electrical conductivity was increased to a value similar to the sample whose CNT concentration and electrically conductive solid content were 15 and 75 wt %, respectively (Figure 3(c)). When the XM-CNT (20 wt %) was replaced by SWCNT, electrical conductivity increased approximately three times, as shown in Figure 3(c). At 35 wt % CNT loading, the composite reaches ~40000 S/m, which is among the highest electrical conductivities ever reported for carbon-based composites.

Unlike electrical conductivity, thermal conductivity is relatively insensitive to CNT and PEDOT:PSS concentrations. A small quantity of CNTs may act as impurities in the polymer matrix and suppress thermal conductivity, but the relatively small increase in thermal conductivity, even at high CNT concentration (15 wt %), is different from the behavior of typical bulks. Figure 4(a) shows that thermal conductivity increases 50% as the CNT concentration is raised from 2 to 15 wt% with 1:4 ratio of CNT to PEDOT:PSS. Conversely, thermal conductivity decreases about 13 wt% when PEDOT:PSS concentration is increased with respect to the fixed 9.8 wt% CNT concentration, as shown in Figure 4(b).

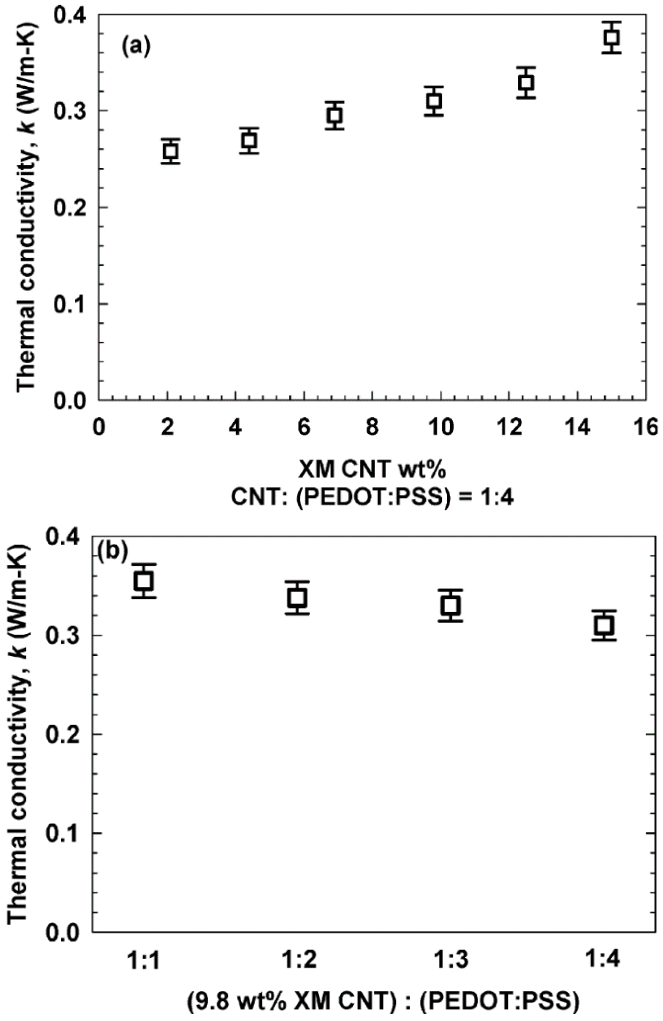

Figure 4. (a) Thermal conductivities of CNT composites at room temperature. (b) Thermal conductivities of the composites with 1:1, 1:2, and 1:3, or 1:4 ratio between CNT and PEDOT:PSS at room temperature. CNT concentration is fixed to 9.8 wt% (reprinted from [45]).

Thermal conductivity (k) of a composite can be described by parallel thermal resistor model as

$$k = k_m V_m + k_f' V_f \quad (2)$$

where k_m and k_f' are thermal conductivities of a matrix and a filler, and V_f represents the volume "fraction" of the indexed (i) material, m (matrix), and f (filler). The measured thermal conductivity of the composite, however, is much smaller than an estimated value, considering thermal conductivities of a typical polymer (k_m) and CNT (k_f') are ~0.2 and ~1000 W/m-K, respectively [6, 7]. For instance, 15 wt% CNT, thermal conductivity is predicted to be ~170 W/m-K, as compared to an actual value of ~0.36 W/m-K. This would be due to thermally poor tube-tube connections, making k_f different from the intrinsic thermal conductivity (k_f') of CNTs.

2.4 Conclusions

A series of segregated-network CNT-polymer composites were prepared, and their thermoelectric properties (electrical conductivity, thermopower, and thermal conductivity) and microstructure were characterized. Composites were made with two different nanotubes (XM-CNT and SWCNT) and stabilizers (PEDOT:PSS and GA) and four different ratios of CNT to PEDOT:PSS, dried at room temperature or/and 80 °C. This study revealed the influence of the most important composite parameters - CNT type and concentration, stabilizer, and drying temperature - on thermoelectric properties. PEDOT:PSS attaches to CNTs and presumably bridges tube - tube junctions. This electrically conducting PEDOT: PSS helps electrons (*i.e.*, holes) to travel more efficiently in the composites, resulting in high electrical conductivity. Thermal transport across the tube - tube junctions, however, is impeded due to mismatches in vibrational spectra between CNT and PEDOT:PSS. This behavior is ideal for developing better

thermoelectric materials. Thermal conductivities of various composites, with 2~15 wt % CNT concentration and 1:1 ~ 1:4 ratios of CNT to PEDOT:PSS, were within those of typical polymeric materials (0.2 ~ 0.4 W/(m-K)). On the other hand, with 35 wt % CNT, electrical conductivity was raised to ~40000 S/m, while thermopower and thermal conductivity remained relatively constant. This electrical conductivity is much greater than those of typical polymer composites containing CNTs. Unlike bulk materials, these composites have thermally disconnected, but electrically connected junctions between conducting particles. The best composites in the present work contains 35 wt % SWCNT and 35 wt % PEDOT:PSS, dried at room temperature and subsequently at 80 °C. This recipe achieved a *ZT* of ~0.02, but may be further increased by using an intrinsically conductive polymer matrix, adding filler materials with high thermopower and electrical conductivity, and varying filler concentrations.

CHAPTER III

LARGE THERMOELECTRIC FIGURE OF MERIT FOR FLEXIBLE ORGANIC COMPOSITES WITH CARBON NANOTUBES*

3.1 Introduction

Inorganic semiconductor materials have been intensively studied for therrmoelectric energy conversion [60-62], but they typically contain heavy, brittle, toxic, expensive elements and require complicated or/and costly manufacturing processes [63]. These disadvantages have been impeded wide use of thermoelectric systems despite their compactness, silence/robustness due to no-moving parts, and versatility in energy harvesting and refrigeration. In this report, carbon nanotube-based organic composites are expected to offer a solution for the drawbacks. Low thermal conductivity of typical organic materials is best suited to thermoelectrics, but their poor electrical properties accompanied by the strong correlation between thermoelectric properties have prevented them as feasible candidates. For instance, when electrical conductivity is raised to a value close to semiconductors, thermopower generally becomes extremely small. However, our approach uses electrically connected, but

* Parts of this section are reprinted from " Light-weight flexible carbon nanotube based organic composites with large thermoelectric power factors," by C. Yu, K. Choi, L. Yin, and J. C. Grunlan, ACS Nano, 5, 7885-7892 (2011) with permission by ACS Nano.

thermally disconnected junctions, making thermoelectric transport properties relative independent. Our composites also have the electrical conductivities higher than ~10^5 S/m, which are orders of magnitude superior to those of typical organic composites. Thermopower was relative kept insensitive ~upon dramatic increases of electrical conductivity while thermal conductivity is maintained within those of organic materials. For instance, composites containing 60-wt% nanotubes and 40-wt% poly (3, 4-ethylenedioxythiophene) poly (styrenesulfonate) yielded ~1.1×10^5 S/m and ~36 μV/K with ~0.2 W/m-K. The loosely related thermoelectric transport properties enabled us to achieve remarkably high *ZT* from fully organic materials up to ~0.2 at 300 K, which is higher than or close to those of inorganic bulk materials such as silicon (*ZT*=~0.01 at 300 K) and PbTe (*ZT*=0.2 ~ 0.3 at 300 K) as well as orders of magnitude higher than those of organic composites. We believe further improvement in thermoelectric properties of the composites may result in an efficiency close to those of commercial inorganic bulk materials (*ZT*=0.7 ~ 0.8 at 300 K). The benefits from organic materials are likely to make them competitive even if their efficiency is lower than those of current inorganic semiconductors.

3.2 Experimental

All samples were made of carbon nanotubes mixed with PEDOT:PSS (Clevios PH500 and PH1000 grades from H.C. Starck) and/or PVAc. The PVAc emulsion is either Vinac XX210 from Ashland Inc. or Vinnapass 401 from Wacker Chemical Co. These two emulsions are 55 solid wt% suspensions in water. The glass transition

temperatures of Vinac XX210 and Vinnapass 401 are approximately 35 and -15 ^{o}C, respectively. Polymer particles in the emulsions have variable sizes ranging from 0.14 to 3.5 μm in diameter with an average diameter of ~650 nm. Purified-grade HiPco single-wall carbon nanotubes were used as conductive fillers in the polymer matrix. The nanotubes were mixed with PEDOT:PSS by sonication with an ultrasonic homogenizer (Misonix Microson XL2000) for 20 min at 50 W. PEDOT:PSS stabilizes nanotubes in water as well as becomes a part of the matrix. The weight ratios of nanotubes to stabilizers were varied from 1:0.25 to 1:1 in order to study the influence of their relative concentrations on transport properties. The viscosity of the aqueous solution was reduced by adding deionized water to the mixture with additional 15 min sonication. Total solids were 2.5 wt % in water for the samples whose nanotube concentrations in fully dried samples are 35, 40, and 45 wt %. For the other samples, 0.4 wt% in water was used due to high viscosity. Then, the emulsion was added to the solution followed by 10 min sonication except for samples 10 and 11. The solution was then poured into a 26 cm^2 container and dried for ~48 h under an ambient condition in a fume hood. Subsequently, the solid composite was baked in an oven at 80 ^{o}C for 6 h. Finally, fully dried composites were stored in a vacuum desiccator for 24 h in order to completely remove residual water from the composites. The thickness of the samples ranges from 0.02 to 0.053 mm. The concentrations of nanotubes, PVAc, and PEDOT:PSS in Table 1 are based on the total dry weight of the composites.

Electrical conductivity and thermopower were measured at room temperature along the in-plane direction. A four-probe current - voltage (I-V) measurement method

was employed to obtain the resistance of the samples so as to extract electrical conductivity by multiplying geometrical factors. Current from 0 to (1 mA was passed to the sample to acquire a slope from a linear I-V curve. For thermopower measurements, voltages across the sample were measured at 10 different temperature gradients between -8 and +8 K. Thermopower was obtained from the slope of a linear temperature - voltage curve. Note that the coefficient of determination (R^2) for finding the slope in the measurement is greater than 0.99.

3.3 Results and discussion

The sample were made of single-wall carbon nanotubes mixed with different grade PEDOT:PSS or/and PVAc polymers. They are black, flexible, and free-standing materials, as shown in Figure 5(b). The concentrations of nanotubes were varied in order to study the effect of nanotube network structure on thermoelectric behavior of the composites.

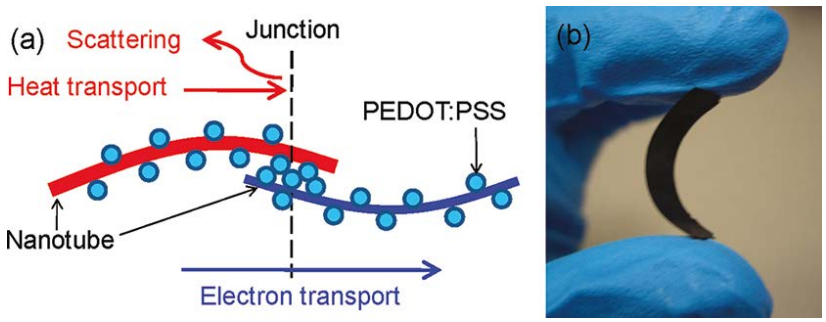

Figure 5. (a) Nanotubes are coated by PEDOT:PSS particles, making nanotube-PEDOT:PSS-nanotube junctions in the composites (b) Fully dried composites held between two fingers indicates that it is a free-standing flexible black material (reprinted from [46]).

Table 1. Concentrations of CNT, PEDOT:PSS, and PVAc for the composites.

Sample	CNT wt%	PEDOT:PSS wt%		PVAc wt%		
		PH500	PH1000	Vinac	Vinnapas	
1	35	35	-	30	-	
2	40	40	-	20	-	
3	45	22.5	-	32.5	-	
4	60	30	-	10	-	
5	70	17.5	-	12.5	-	
6	75	18.75	-	6.25	-	DMSO
7	60	30	-	-	10	
8	60	-	30	10	-	
9	60	-	30	-	10	
10	60	40	-	-	-	
11	60	-	40	-	-	

The electrical conductivities of the samples are shown as red filled circles in Figure 6 when the nanotube concentrations were varied from 35 to 75 wt%. The ratio of nanotubes and PH500 grade of PEDOT:PSS was 1:1 for 35 and 40 wt% samples, 1:0.5 for 45 and 60 wt% samples, and 1:0.25 for 70 and 75 wt% samples. The electrical conductivity was gradually increased by raising the nanotube concentration up to 60 wt%. However, additional nanotubes used in 70 and 75 wt% composites suppressed the electrical conductivity. With 35 and 60 wt% of nanotubes, electrical conductivities were measured to be 4.71×10^4 and 1.35×10^5 S/m, respectively, which are orders of

magnitude higher than those of typical nanotube-filled polymer composites.[10, 58, 59] The electrical conductivities of nanotube-only networks may be calculated as ~10^5 S/m by considering the nanotube network and the polymer as parallel resistors. This conductivity is close to recent measurement results for the films made of only nanotubes [47], which provides an indirect evidence of good electrical pathways across nanotube junctions.

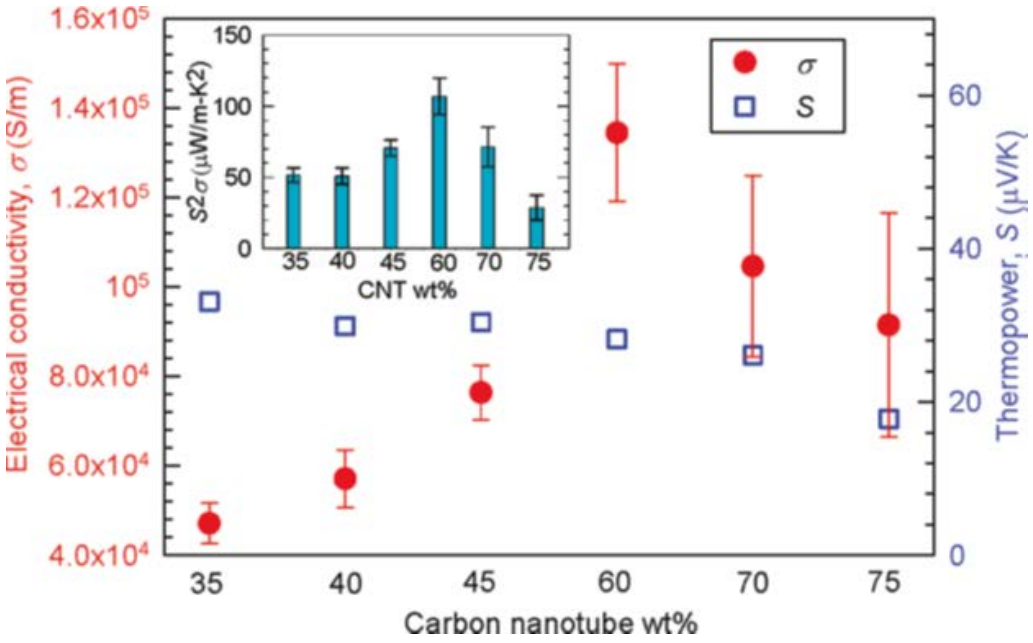

Figure 6. Electrical conductivities (red circles) and thermo powers (blue squares) of the composites with different nanotube concentrations. The inset shows the thermoelectric power factors ($S^2\sigma$) (reprinted from [46]).

The electrical conductivities of the samples are shown as red filled circles in Figure 6 when the nanotube concentration was varied from 35 to 75 wt%. The ratio of nanotubes and PH500 grade of PEDOT:PSS was 1:1 for 35 and 40 wt% samples, 1:0.5

for 45 and 60 wt% samples, and 1:0.25 for 70 and 75 wt% samples. The electrical conductivity was gradually increased by raising the nanotube concentration up to 60 wt%. However, additional nanotubes used in 70 and 75 wt% composites suppressed the electrical conductivity. With 35 and 60 wt% of nanotubes, electrical conductivities were measured to be 4.71×10^4 and 1.35×10^5 S/m, respectively, which are orders of magnitude higher than those of typical nanotube-filled polymer composites [10, 58, 59]. The electrical conductivities of nanotube-only networks may be calculated as $\sim 10^5$ S/m by considering the nanotube network and the polymer as parallel resistors. This conductivity is close to recent measurement results for the films made of only nanotubes [47], which provides an indirect evidence of good electrical pathways across nanotube junctions.

It is worth pointing out that the intrinsic electrical conductivity of an "individual" nanotube considerably varies between 10^1 and 10^7 S/m at room temperature depending on the chirality [28]. Bulk-scale composites contain various chirality nanotubes whose intrinsic electrical characteristics are either metallic or semiconducting. Nevertheless, when nanotubes are exposed to air (particularly for nanotubes made in an oxygen-rich environment like our sample preparation processes with aqueous solutions), semiconducting nanotubes become degenerate p-type conductors [47, 64-66], making less electrically resistive paths across the junctions. The work functions of both metallic and semiconducting nanotubes become ~5.0 eV after doping [64], which matches that of PEDOT:PSS. In doping experiments, we also observed that the electrical conductivity of nanotube-only films was significantly decreased when nanotubes were annealed in

vacuum, but the conductivity was recovered when they were exposed to air. The reduction in the electrical conductivity from the samples containing more than 60 wt % nanotubes could be attributed to less effective nanotube dispersion due to the lack of the stabilizer (PEDOT:PSS). PEDOT: PSS coats the surface of nanotubes, playing an important role in separating bundled/clumped nanotubes into smaller bundles or individual tubes in water as well as binding them to form composites upon drying. Bundled and aggregated nanotubes due to the lack of dispersants lessen the number of nanotube connections responsible for electron transport. The electrical conductivity of the doped samples (75 wt % nanotube) was also decreased, although the electrical conductivity of PEDOT:PSS was improved by DMSO doping. In addition to the inferior dispersion, insufficient polymeric binding materials in doped sample (75 wt % nanotube) are likely to be partly responsible for the suppression. This influence is also reflected in the thermopower lower than 20 μV/K. Note that typical PEDOT:PSS films show ~10 μV/ K [24, 33, 67], and a composite made of DMSO-doped PEDOT: PSS (30 wt %) and electrically insulating PVAc has only 17 μV/K at room temperature [45]. It is striking that thermopowers of samples with low CNT concentration (35 ~ 60 wt %) were high and consistent (28 ~ 33 μV/K) even with the very high and 3-fold increase in the electrical conductivity (from 4.71×10^4 to 1.35×10^5 S/m). The power factor was calculated to be up to~100 μW/m-K^2, as plotted in the inset of Figure 6.

When we assume the nanotubes formed random three-dimensional (3D) networks, the thermal conductivity ($k_{3D,NT}$) may be calculated using Eq (3) [68].

$$k_{3D,NT} = \frac{G}{R}\frac{\pi(nL^2R)^2}{36}\left(1+16\left(\frac{R}{L}\right)+80\left(\frac{R}{L}\right)^2+192\left(\frac{R}{L}\right)^3+153.6\left(\frac{R}{L}\right)^4\right) \quad (3)$$

where G, R, n, and L indicates thermal contact conductance between nanotubes, the radius of nanotubes, the volume number density of intertube contacts, and the length of nanotubes, respectively. The volume number density, n, is equal to $\rho/(2\pi RLn_\sigma m)$, where ρ, n_σ, and m indicate density (~1.1 g/cm^3) [69], the number density of carbon atoms on the surface of a nanotube, and the mass of a carbon atom, respectively. In our experiments, the average nanotube length and diameter are ~550 nm and ~1 nm, respectively, according to the specification from the manufacturer. Figure 7 shows the calculated thermal conductivity (k_{3D}) of a composite made of a 3D nanotube network ($k_{3D,NT}$) and polymers (k_m) with Eq (1) and (2) when G varies from 0.1 to 100 pW/m-K.

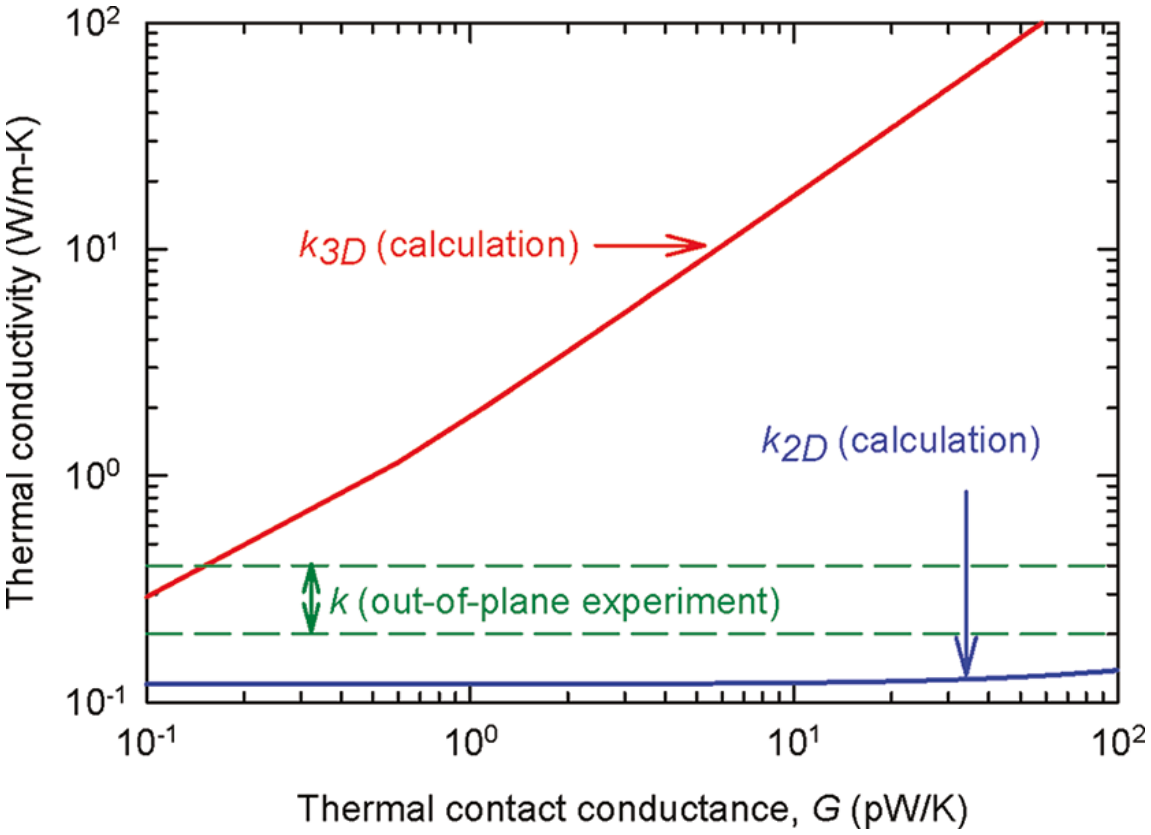

Figure 7. Theoretical thermal conductivity (k_{3D}) of a composite containing a 3D nanotube network and the theoretical out-of-plane thermal conductivity (k_{2D}) of a composite containing 2D nanotube network when thermal contact conductance varies from 0.1 to 100 pW/K. The out-of-plane experimental thermal conductivity ranges from 0.2 to 0.4 W/m-K. For calculations, nanotube vol% and the polymer thermal conductivity were set to be 60 and 0.3 W/m-K, respectively, and the parallel resistor model was used (reprinted from [46]).

The plotted values also match the results that we calculated by using the model provided Chalopin et al [70]. The out-of-plane thermal conductivity (k_{2D}) of a composite made of 2D nanotube networks ($k_{2D,NT}$) and polymers (k_m) may be considered as a lower bound since it is unlikely that we have a composite structure made of stacked 2D layers. This structure has a very low out-of-plane thermal conductivity due to small thermal contact conductance between each layer. The $k_{2D,NT}$ may be calculated using Eq (4) [68].

$$k_{2D,NT} = \frac{2G}{\pi}\left(\frac{\rho(2R+h)}{2\pi(R/L)n_{\sigma}m}\right)(2R+h) \quad (4)$$

where h indicates the equilibrium distance between the surfaces of parallel nanotubes; k_{2D} is more or less invariant ~0.1 W/m-K due to very small $k_{2D,NT} \sim 10^{-2}$ W/m-K. Our experimental results are closer to k_{2D} than k_{3D}, which may suggest that some nanotubes were embedded into the composites in the in-plane direction. When the samples were dried from aqueous nanotube mixtures, nanotubes are likely to be pushed to the bottom by the water surface.

3.4 Conclusions

The composites in this research containing polymers and carbon nanotubes without containing heavy and/or toxic inorganic materials exhibited very high electrical conductivities and relatively constant thermopowers. The thermopowers were weakly correlated with the electrical conductivities, resulting in large thermoelectric power factors ($S^2\sigma$), ~160 μW/m$^-$K^2, which are orders of magnitude better than those of typical polymer composites. The optimum nanotube concentrations for better power factors were identified to be 60 wt%. The highest electrical conductivity and thermopower along the in-plane direction of our samples were recorded to be 1.35×10^5 S/m and 41 μV/K at room temperature, respectively. Without additional DMSO doping, PH1000 shows higher thermopowers while PH500 has better electrical conductivities. The thermal conductivity in the out - of - plane direction was measured to be 0.2 ~ 0.4 W/m-K at

room temperature. The in - plane thermal conductivity and thermal contact conductance between nanotubes in our composites were also theoretically estimated. It is believed further research utilizing the loosely related transport properties may enable us to obtain easy-to-manufacture, low cost, light-weight, and less toxic organic composites for efficient thermoelectric energy conversion in the future.

CHAPTER IV

HIGHLY DOPED CARBON NANOTUBES WITH GOLD NANOPARTICLES AND THEIR INFLUENCE ON ELECTRICAL CONDUCTIVITY AND THERMOPOWER*

4.1 Introduction

Carbon nanotubes (CNTs) are often used as conductive fillers in composite materials, but electrical conductivity is limited by the maximum filler concentration that is necessary to maintain composite structures. This paper presents further improvement in electrical conductivity by precipitating gold nanoparticles onto CNTs. In the composites in this research, the concentrations of CNTs and poly (vinyl acetate) were respectively 60 and 10 vol%. Four different gold concentrations, 0, 10, 15, or 20 vol% were used to compare the influence of the gold precipitation on electrical conductivity and thermopower of the composites. The remaining portion was occupied by poly(3,4-ethylenedioxythiophene) poly(styrenesulfonate), which de-bundled and stabilized CNTs in water during synthesis processes. The concentrations of gold nanoparticles are below the percolation threshold of similar composites. However, with 15-vol% gold, the electrical conductivity of our composites was as high as ~6×10^5 S/m, which is at least ~500 % higher than those of similar composites as well as orders of magnitude higher

*Parts of this section are reprinted from "Highly doped carbon nanotubes with gold nanoparticles and their influence on electrical conductivity and thermopower of nanocomposites," by K. Choi, and C. Yu, PLos One, 7, e44977 (2012) with permission by PLos One.

than those of other polymer composites containing CNTs and gold particles. According to our analysis with a variable range hopping model, the high conductivity can be attributed to gold doping on CNT networks. Additionally, the electrical properties of composites made of different types of CNTs were also compared.

4.2 Experimental

Three different-type CNTs were used: SWCNTs synthesized by a high pressure carbon monoxide (HipCo) process (HSWCNT) [71] and a chemical vapor deposition (CVD) method (CSWCNT) [72] as well as multi-wall carbon nanotubes (MWCNT) by a CVD method [73]. CNTs were added to deionized water (~20 ml), and the solution was sonicated with an ultrasonic homogenizer (Microson XL2000, Misonix, Inc.) for 30 minutes with 50 W power. A gold ion solution was separately prepared by adding chloroauric acid ($HAuCl_4$, Alfa Aesar, 99.9%) to deionized water (1~2 ml), and then poured into the CNT solution, followed by 30 min sonication. Subsequently, an aqueous poly (3, 4-ethylenedioxythiophene) poly (styrenesulfonate) (PEDOT:PSS, Clevios PH1000, H. C. Starck) solution was added to the mixture, followed by 15 min sonication. PEDOT:PSS plays a role in de-bundling and dispersing CNTs in water. Finally, poly (vinyl acetate) (PVAc) emulsions were added to the mixture, followed by another 15 min sonication. Two different PVAc emulsions, Vinnapas 401 and 600BP (Wacker chemical, Co.) were used. They have different glass transition temperatures (T_g): -15 and -40 ^{o}C for Vinnapas 401 and 600BP, respectively. The polymer particles in the emulsion vary in size from 0.14~3.5 μm in diameter with an average diameter of

~650 nm. The total weight including water is typically 25 g. The aqueous mixture was then poured into a 26 cm^2 plastic container and dried for 48 hrs under an ambient condition in a fume hood. During the drying process, the plastic container was placed on a rotating turntable (3 rpm). Sidewalls were made on the turntable in order to avoid non-uniformity of the solid contents due to air flow in the fume hood. The solid composite was then baked in a vacuum oven at 80 ^oC for 2 or 6 hrs. The baking process helps making strong binding between nanotubes and polymers as well as removing micro voids in the composite. Finally, fully dried composites were placed in a vacuum desiccator for 24 hs in order to completely remove residual water from the composite. The thickness of the composite ranged from 27 to 40 μm.

Table 1 shows a list of samples and vol% of the materials in the composite. The actual weights of the materials are the following. For the samples containing SWCNTs with 10-, 15-, and 20-vol% gold, the weights of $HAuCl_4$ respectively were 0.1094 g, 0.1263 g, and 0.1368 g; the weights of CNT respectively were 0.0256 g, 0.0197 g, and 0.0160 g; the weights of PH1000 respectively were 0.4648 g, 0.2682 g, and 0.1453 g; the weights of PVAc respectively were 0.0071 g, 0.0055 g, and 0.0044 g. The solid contents of the aqueous PH1000 [74] and PVAc [7] solutions respectively were 1.5 and 55.16 wt%. The densities of gold [75], SWCNT [76], PH1000 [74], PVAc [7] used for calculating vol% respectively were 19.3, 1.3, 1.06, and 1.19 g/cm^3. The density of MWCNT is 2 g/cm^3 [77], which is different from that of SWCNT. Due to the difference, the contents of the samples containing MWCNT were not the same as those of SWCNT samples. For the sample 9, the weights of MWCNT, $HAuCl_4$, PH1000, and

PVAc were 0.0274 g, 0.1141 g, 0.2424 g, and 0.0049 g, respectively. The samples without gold were also prepared with SWCNT and MWCNT. In sample 8, 0.0641 g of CNT, 1.7420 g of PH1000, and 0.0177 g of PVAc were mixed, whereas 0.0733 g of MWCNT, 1.2951 g of PH1000, and 0.0132 g of PVAc were used in sample 7.

Table 2. List of the composites with all contents and their vol%. Three different CNT type and two different PVAc were used with varying gold nanoparticle concentrations. The samples were synthesized by drying aqueous mixtures at room temperature for 48 hrs and subsequently at 80 ^{o}C for 2 or 6 hrs.

Sample number	CNT type	CNT vol%	PEDOT:PSS vol%	Au vol%	PVAc vol%		Drying time (hr) at 80 ^{o}C
					401	600BP	
1	HSWCNT	60	20	10	10	-	2
2	HSWCNT	60	15	15	10	-	2
3	HSWCNT	60	10	20	10	-	2
4	HSWCNT	60	20	10	-	10	6
5	HSWCNT	60	15	15	-	10	6
6	HSWCNT	60	10	20	-	10	6
7	MWCNT	60	30	-	-	10	6
8	CSWCNT	60	30	-	-	10	6
9	MWCNT	60	15	15	-	10	6
10	CSWCNT	60	15	15	-	10	6

Electrical conductivity was obtained by a four-point probe method (current-voltage sweeping) and thermopower was acquired by measuring temperature differences and voltages across the samples at room temperature. The error bars were obtained from 2-4 measurements and uncertainties associated with dimensions (length, width, and thickness of the samples) and thermocouple reading. Errors were calculated with error

propagation methods [78]. For electron microscopy analysis, the composites were cold-fractured by submerging the composites in liquid nitrogen for 5 min, and then the cross section of the composites was inspected.

4.3 Results and discussion

All samples contain 60-vol% CNTs and 10-vol% PVAc, and the rest 30 vol% was PEDOT:PSS or PEDOT:PSS with gold (2:1, 1:1, and 1:2 ratios), as listed in Table 2. For the samples containing SWCNT (Sample #: 1~6), many nanotubes in the sample with 20-vol% PEDOT:PSS were embedded (Figure 8(a)) whereas the samples with 15- and 10-vol% PEDOT:PSS show more nanotubes separated from the polymer (Figure 8(b) and 8(c)), presumably due to less stabilizers. Gold nanoparticles were observed in the sample with 20-vol% gold (Figure 8(c)). Two PVAc polymer with different T_g (Vinnapas 401 and 600BP) were used, but we did not find any noticeable differences in microstructures.

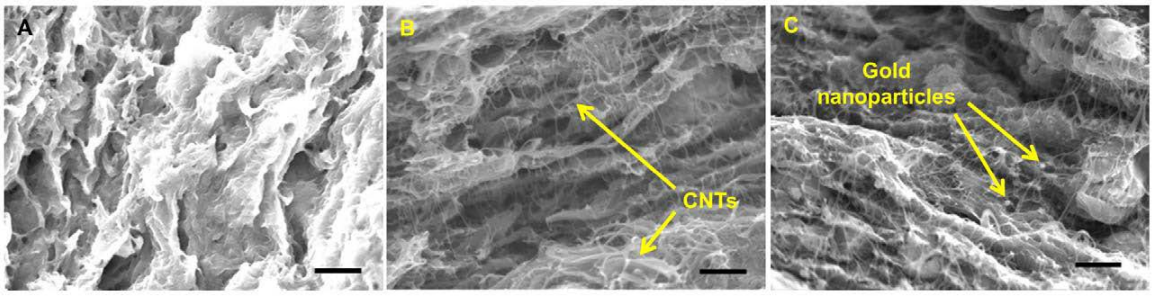

Figure 8. Cold-fractured cross sections of samples with 10, 15, and 20-vol% of gold nanoparticles. With increasing PEDOT:PSS vol%, more CNTs were pulled out from the surface. The arrows indicate CNTs and gold nanoparticles. All scale bars indicate 1μm (reprinted from [79]).

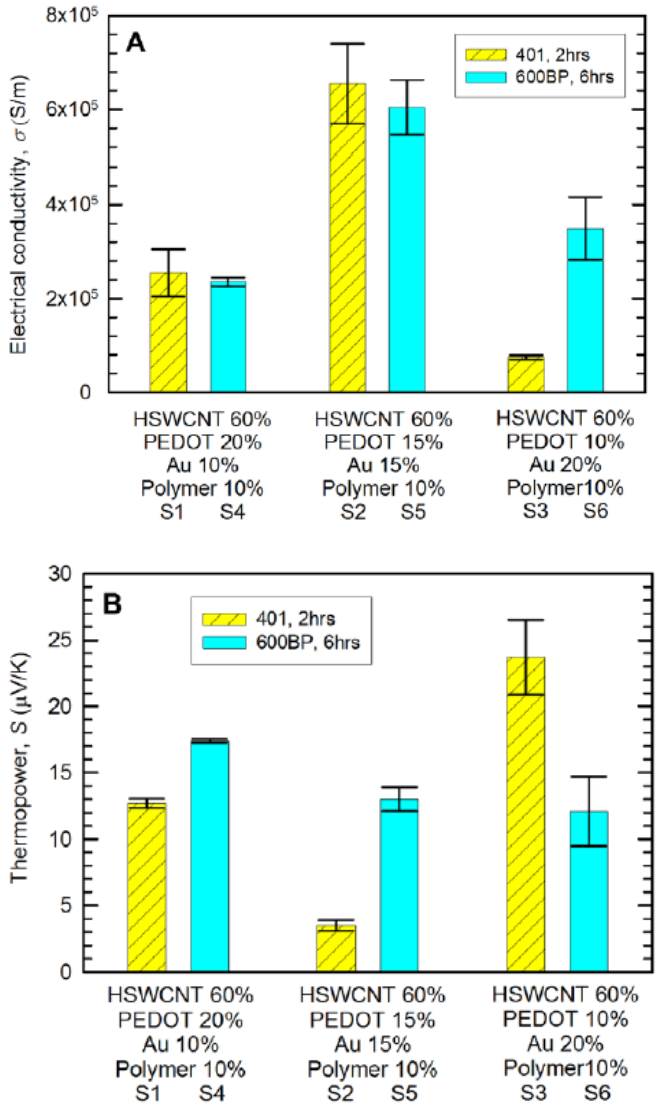

Figure 9. Electrical conductivity (a) and thermopower (b) of samples. The vol% of HSWCNT and polymer (Vinnapas 401 or BP600) was 60 and 10. The ratio of PEDOT:PSS to gold was 2:1, 1:1, or 1:2 (reprinted from [79]).

Figure 9(a) shows the electrical properties of Sample 1~6. The electrical conductivity was increased when the gold content was increased from 10 (Sample 1 and 4) to 15 vol% (Sample 2 and 5). The highest electrical conductivity was measured to be

~6×10^5 S/m with 15-vol% PEDOT:PSS, 15-vol% gold, and 60-vol% SWCNT. This value is orders of magnitude higher than those of other nanotube-filled polymer composites [43, 44] and shows ~500 % improvement compared to our previous work with similar amounts of SWCNT and PH1000 (~9×10^4 S/m) [46]. It is likely that the electrical conductivity of gold is not the only reason that we obtained such high electrical conductivity from the composites. This is because the typical percolation threshold of gold nanoparticles is ~30 vol% in polymer composites [80], which is larger than the maximum gold concentration (20 vol%) in our experiments. In other words, when the concentration of the nanoparticles is lower than the percolation threshold, the mean distance between the nanoparticles is too large to have connected gold networks. For example, Devasdoss et al. showed that the maximum conductivity is 8×10^{-8} S/m with a composite containing gold nanoparticles (mole ratio of 4.95×10^{-2}) and metallopolymer [81]. Podhaecka et al. reported that the electrical conductivity of a composite with gold nanoparticles (~10 vol%) and poly(3-octylthiophene) is 10^{-4} S/m [82]. A high gold nanoparticle concentration, 40 vol% well above the percolation threshold in poly-4-vinyl pyridine matrices resulted in only ~10^2 S/m [80]. Such lower electrical conductivities suggest the high electrical conductivity from our samples is likely from p-type doping on nanotubes by the nanoparticles.

Gold nanoparticles are easily precipitated by spontaneous reduction [42, 52] due to the larger reduction potential of gold ions ($[AuCl_4]^- + 3e^- \rightarrow Au(s) + 4Cl^-$, standard electrode potential (E^0) = +0.93~1.002V) [47, 83-85] than those of nanotubes [47]. This causes nanotubes to donate electrons to gold, thereby increasing hole carrier

concentrations [86, 87]. The work functions of SWCNTs (4.5~5.0 eV) [88, 89] and MWCNTs (4.3~4.95 eV) [88, 90] are also smaller than that of gold (5.1~5.47 eV [91, 92]), making electrons transferred from nanotubes to gold nanoparticles. The electrical conductivity of the sample with 20-vol% gold (sample 3 and 6) is lower than those of the samples containing 15-vol% gold. The inferior conductivity with the higher gold concentration also suggests that gold nanoparticles themselves did not make percolated paths or significantly affect the electrical conductivity of our composites. We believe this is due to the poor nanotube dispersion caused by the small volume fraction of PEDOT:PSS, which de-bundles and disperses carbon nanotubes in water. When large carbon nanotube bundles are present in the composites, the number of tube-tube junctions decreases, resulting in electrically more resistive nanotube networks [46, 93]. Furthermore, the composite contains more pores because large bundles are not readily embedded in the polymer due to increased stiffness.

Two different annealing conditions (2 hrs and 6 hrs at 80^{o}C) were tested to identify any changes in electrical properties. The longer annealing time made the sample mechanically stronger but the electrical conductivities of the samples containing 10- or 15-vol% gold are not strongly dependent on the drying condition. When the gold concentration was increased to 20 vol% (S3 and S6), the longer drying time resulted in a higher electrical conductivity. Sample 3 was particularly weaker than Sample 6, which may have affected the electrical conductivity. It should be noted that the PVAc did not alter the electrical properties significantly. Two different composites containing 60-wt%

SWCNT and 30-wt% PH1000 with 10-wt% PVAc showed similar conductivities, ~9×10^4 S/m for Vinnapas 401 and ~8.4×10^4 S/m for Vinnapas BP600.

Figure 9(b) depicts thermopower values of Sample 1~6, which were inversely proportional to the electrical conductivities. These values are lower than those of the samples containing 60 wt% SWCNT (30~40 μV/K) [46], but higher than that of gold (1.94 μV/K at room temperature) [94]. This is another evidence that gold nanoparticles were not percolated. Sample 2 has the smallest thermopower value, which may be due to the highest electrical conductivity and shorter annealing time (mechanically weaker than Sample 5). We believe that the smaller thermopower than those of similar composites without gold can be attributed to doping.

Here, we analyzed that the influence of the gold doping on the electrical conductivity of the nanotube networks. The electrical conductivity of a composite with a high nanotube loading can be analyzed with a parallel resistance model [46, 95] and the variable range hopping model [10, 96]. The parallel resistance model describes the electrical conductivity (σ_c) of a composite:

$$\sigma_c = \phi_{CNT}\sigma_{CNT} + \phi_{PEDOT}\sigma_{PEDOT} + \phi_{polymer}\sigma_{polymer} \quad (5)$$

where σ_{CNT}, σ_{PEDOT}, and $\sigma_{polymer}$ are the electrical conductivity of nanotube networks in the composite, PEDOT:PSS, and PVAc, respectively. Also, ϕ denotes the volume fraction of each material. Here, $\sigma_{polymer} \approx 0$ because the PVAc polymer is electrically insulating (less than 10^0 S/m) whereas the value of σ_{PEDOT} was directly measured with 100% of PEDOT:PSS film (~10^2 S/m, without dimethyl sulfoxide (DMSO) doping). Note that the electrical conductivity of PEDOT:PSS film doped with 5 wt% of DMSO

was reported as ~10^4 S/m [97-99]. In our experiments, PEDOT:PSS was not doped with DMSO in order not to reduce thermopower of PEDOT:PSS. The nanotubes in our composites can be assumed to be three dimensional (3D) networks and the electrical conductivity of nanotube mat, σ_{CNT}, can be described by the 3D variable range hopping model [10, 96].

$$\sigma_{CNT}(T) = \sigma_o \exp\left[-\left(\frac{T_1}{T}\right)^{1/1+d}\right] \tag{6}$$

σ_o is a constant, which represents the saturated electrical conductivity of nanotube networks when the temperature effect on electron carriers is negligible at infinite temperature. T_1 is related to the energy barrier for electron hopping through tube-tube junctions. T is temperature. When d=3, it represents bulk conduction of pure carbon nanotube mats [96]. The major difference between σ_{CNT} and σ_o comes from tube-tube junctions. σ_{CNT} is for CNT networks with polymers between nanotube junctions whereas σ_o is for pure tube-tube junctions without any materials in between (intrinsic properties without considering the junction effects). Therefore, it is possible to obtain the influence of the p-type doping on the electrical conductivity of the nanotube networks by comparing σ_o with (indicated by Au subscript) and without (indicated by NoAu subscript) gold nanoparticles, as shown in the following equations.

$$\sigma_{o,NoAu} = \sigma_{CNT,NoAu} \exp\left[-\left(\frac{T_1}{T}\right)^{\frac{1}{4}}\right]^{-1}, \quad \sigma_{o,Au} = \sigma_{CNT,Au} \exp\left[-\left(\frac{T_1}{T}\right)^{\frac{1}{4}}\right]^{-1} \tag{7}$$

The normalized factors can be obtained from $\sigma_{o,Au}/\sigma_{o,NoAu}$, and it is possible to estimate the influence of the gold doping on electrical conductivity. From Eq. (7), the normalized factor is;

$$\frac{\sigma_{o,Au}}{\sigma_{o,NoAu}} = \frac{\sigma_{CNT,Au}}{\sigma_{CNT,NoAu}} \tag{8}$$

The normalized factor is independent of T_1 or d. Here, the electrical conductivity of nanotube networks, $\sigma_{o,NoAu}$ was referred from the electrical conductivity of HSWCNT mats (~2.5×10^5 S/m at room temperature, highest conductivity from SWCNT mats, to our best knowledge) [100]. The composites with similar compositions in previous work [46] were analyzed to obtain T_1 values as a function of nanotube concentration at 300K. Here, PEDOT:PSS were also used to de-bundle and stabilize CNTs in water, making tube-tube junctions similar to those of the composites in this study. The composites contain 35~75 wt% SWCNTs with PEDOT:PSS and PVAc. The carbon nanotube wt% was converted into vol% and plotted in Figure 10(a) (hollow square) because the density of gold used in this work is one order higher than the polymers and CNTs. The conversion enables us to properly compare properties of the composites containing the same CNT concentrations, as described below. Then, the composite electrical conductivity (σ_c) in Eq. (5), as shown in Figure 10(a) (filled circles), was used with σ_{CNT} in Eq. (6) to find T_1. Here, T_1 at 60 vol% SWCNT concentration was obtained to be 6.06K from the linear interpolation of 54.6 vol% (60 wt%) and 65.8 vol% (70 wt%).

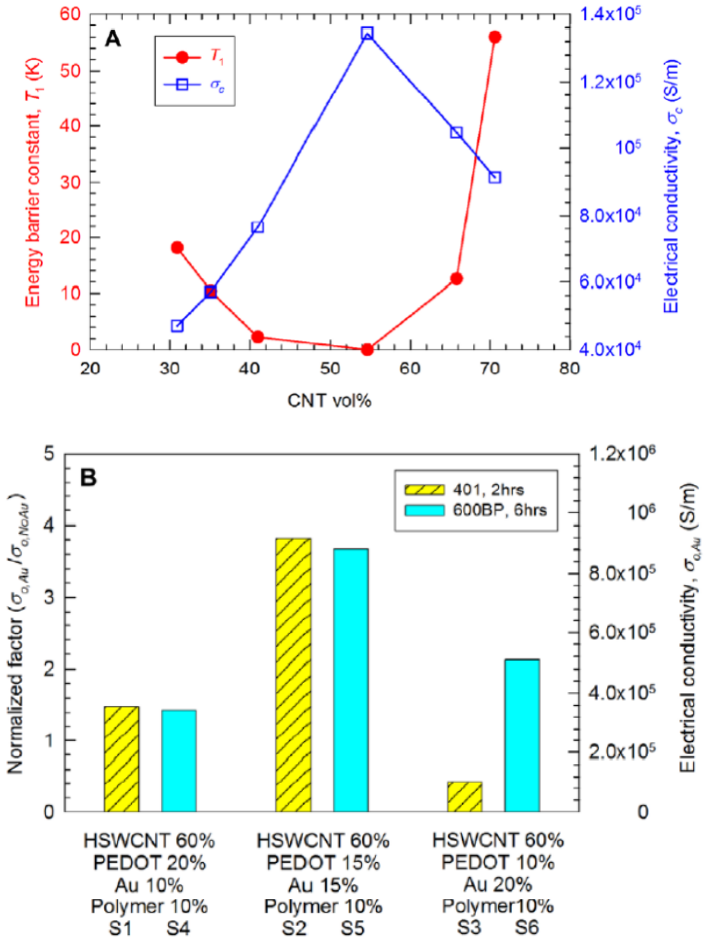

Figure 10. (a) The energy barrier constant, T_1 in Eq. (6) as a function of CNT vol% (red filled circles). (b) The normalized factor ($\sigma_{o,Au}/\sigma_{o,NoAu}$) that indicates the effect of gold doping for CNT networks and electrical conductivity of gold-incorporated CNT networks ($\sigma_{o,Au}$). T_1 was found from the electrical conductivities (σ_c) of similar composites (blue hollow squares) containing 60-wt% HSWCNT, 30-wt% PEDOT:PSS, 10-wt% PVAc from our previous work [46]. For $\sigma_{o,Au}$ and $\sigma_{o,NoAu}$, tube-tube junction resistances in CNT networks were not considered (reprinted from [79]).

When we assume the tube–tube junctions are similar after the gold nanoparticle incorporation, T_1 values can be used for our composites in this study. Then, we can estimate the electrical conductivity of the gold-decorated nanotubes by using Eq. (5) and (6). In other words,

$$\sigma_{o,Au} = \frac{\left(\sigma_c - \sigma_{PEDOT}\phi_{PEDOT}\right)}{\phi_{CNT}} \exp\left[-\left(\frac{T_1}{T}\right)^{\frac{1}{4}}\right]^{-1} \quad (9)$$

Figure 10(b) depicts the normalized factor (left y axis), which describes the electrical conductivity normalized by the values without gold doping ($\sigma_{o,Au}/\sigma_{o,NoAu}$). The electrical conductivity of the nanotube network with 15-vol% gold nanoparticles was increased by a factor of ~4. However, the electrical conductivity of the composite with 20 vol% of gold nanoparticles (Sample 3) was decreased, presumably due to poor nanotube dispersions caused by a lack of the dispersant (PEDOT:PSS) and the high concentration of gold nanoparticles.

We also used different types of nanotubes (MWCNT or CSWCNT) to identify the influence of the nanotubes on the electrical properties. Samples with 60-vol% CNT, 30-vol% PEDOT:PSS, and 10-vol% polymer emulsion (Vinnapas 600BP) were prepared without gold (Sample 7 and 8). With 15-vol% gold, PEDOT:PSS was reduced to 15 vol% (Sample 9 and 10). We found that MWCNT/CSWCNT-composites containing 15-vol% gold have higher electrical conductivities, compared to the composites containing 10 and 20-vol% gold. Sample 7 and 8 (without gold) show relatively smooth and uniform cross sections. More nanotubes were pulled out from the polymer with CSWCNTs (Figure 10(b)) than MWCNTs. This may be from inferior dispersions (i.e., more aggregations) of MWCNTs compared to SWCNTs as well as from shorter lengths of MWCNTs (1~12 μm) [73] than SWNTs (5~30 μm) [72]. Additionally, the number of MWCNTs is less than that of SWCNTs due to the higher density of MWCNTs. With 15-vol% gold, relatively large gold particles were observed (Figure 11(c) and 11(d)). From

the energy dispersive X-ray Spectroscopy analysis, it was confirmed that the particles are comprised of gold.

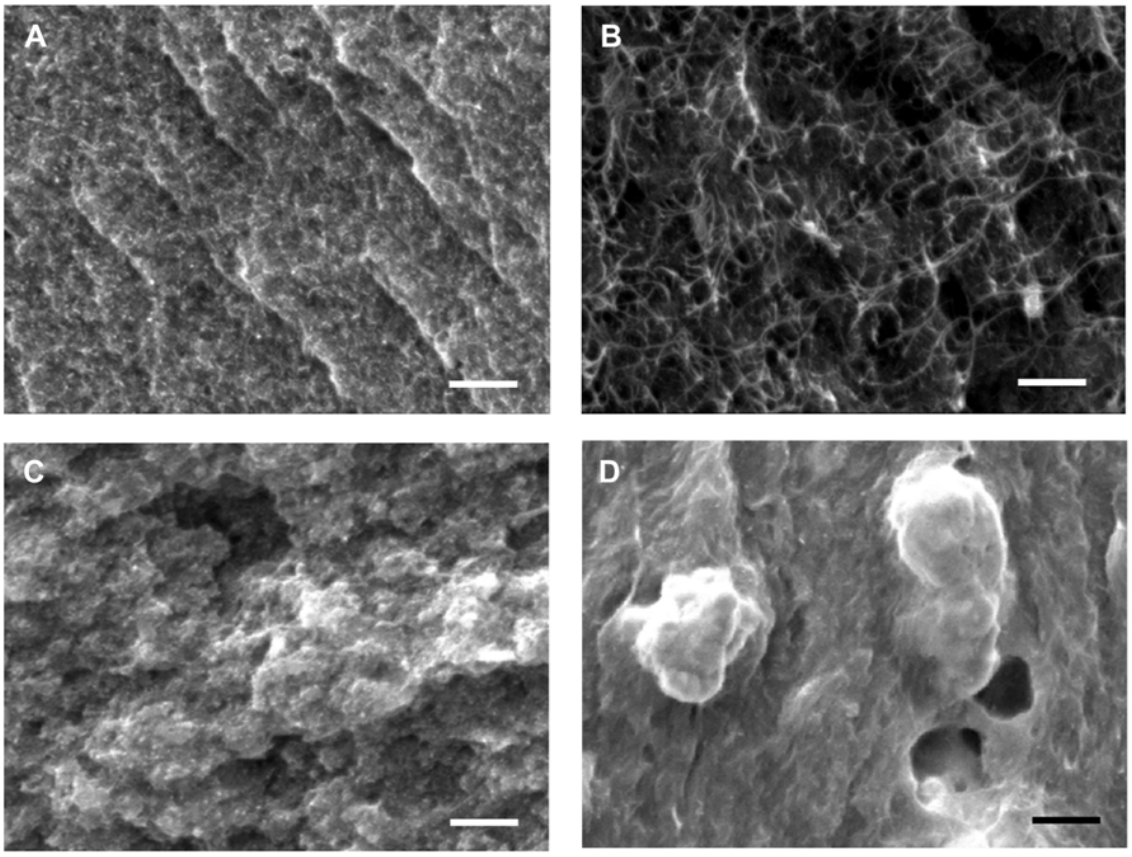

Figure 11. Cold-fractured cross sections of sample 7 (a), sample 8 (b), sample 9 (c), and sample 10 (d) (see Table 2) (reprinted from [79]).

The electrical conductivities of the composites containing three different types of nanotubes were compared in Figure 12(a). The composite with MWCNT shows ~4×10^3 S/m, which is inferior to that of the HSWCNT sample (~2×10^4 S/m). In CNT networks, the electrical conductivity is often governed by tube-tube junctions [93]. When MWCNTs are used, the number of the junctions is small compared to those of SWCNT networks, diminishing electrons transport across the junctions. The large

diameter of MWCNTs causes much smaller surface areas than SWCNTs. Moreover, the aggregation of MWCNTs can also be attributed to the inferior conductivity of the MWCNT sample. After replacing 15-vol% PEDOT:PSS with 15-vol% gold in these composites, the electrical conductivities were dramatically increased to ~7×10^4 and ~9×10^4 S/m for the MWCNT/gold and CSWCNT/gold samples, respectively. Nevertheless, these values are still lower than that of the HSWCNT/gold sample. It has been reported that the intrinsic electrical conductivity of HSWCNT is higher than that of CSWCNT (approximately one order difference) [101], generally due to the higher concentration of metallic nanotubes in HSWCNT [101]. In addition, the presence of more defects such as carbonaceous particles on the surface of the CSWCNT compared to HSWCNT may cause an increase in the contact resistance between nanotubes [102]. The large difference in the electrical conductivities of the composites with CSWCNT and HSWCNT also shows that CNT networks are the electron paths rather than gold nanoparticles. Note that the electrical conductivity of bulk gold (~4×10^7 S/m at 300K) [75] is at least two-order higher than that of our composites containing CSWCNT and 15-vol% gold. The thermopower values of the composites with gold nanoparticles were measured to be less than a half of those without gold, due to the large improvement in electrical conductivity by p-doping of CNT (Figure 12(b)).

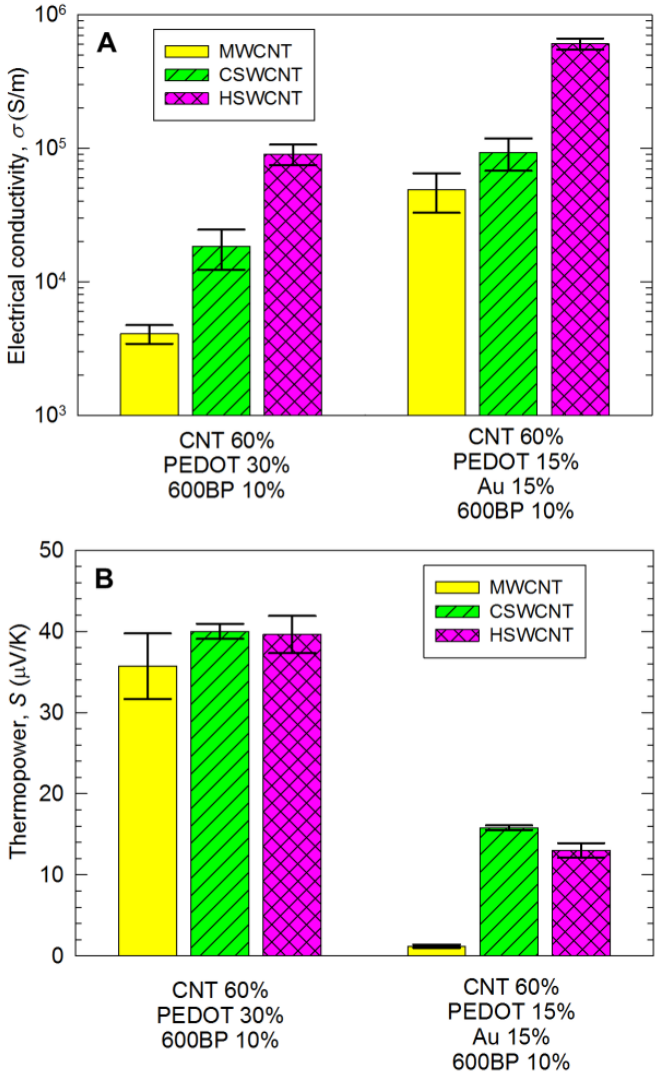

Figure 12. Electrical conductivity (a) and thermopower (b) of sample 7~10 along with those of sample 5 and a sample in Ref [46] for comparison (reprinted from [79]).

4.4 Conclusions

Polymer composites containing SWCNTs grown by a HipCo or CVD process or MWCNTs with PEDOT:PSS and PVAc. The vol% of CNT and PVAc was 60 and 10, respectively. The concentration of gold nanoparticles was 0, 10, 15, and 20 vol%, and

the rest was occupied by PEDOT:PSS. Their electrical conductivities and thermopower values were measured for the composites without and with gold nanoparticles for doping CNTs. With the doping, the electrical conductivity of the composites was dramatically increased to ~6×10^5 S/m by replacing 15-vol% PEDOT:PSS with gold nanoparticles. This electrical conductivity is orders of magnitude higher than those of other polymer composites containing CNTs and gold particles. Furthermore, the conductivity is ~500 % higher than those of similar composites without gold nanoparticles. We believe this is due to p-type doping caused by gold nanoparticles when they are precipitated on CNTs. A variable range hopping model with a parallel resistance model was employed to identify the change in the electrical conductivity of CNT networks in the composites. We also observed that the composites containing 20-vol% gold nanoparticles decreased the electrical conductivity due to the inferior CNT dispersions. This result indicates CNT dispersion with a proper amount of CNT dispersants is crucial to maximize electrical conductivity. Additionally, three different CNTs resulted in dissimilar electrical properties for the composites, showing that the intrinsic properties of the CNTs and dispersion are important factors. This study demonstrates nanoparticles can be used for doping CNTs to manipulate the electrical properties of CNT-filled polymer composites.

CHAPTER V

N-TYPE THERMOELECTRIC PERFORMANCE OF CARBON NANOTUBE-FILLED POLYMER COMPOSITES*

5.1 Introduction

Carbon nanotubes (CNTs) were functionalized with polyethyleneimine (PEI) and made into composites with polyvinyl acetate (PVAc). CNTs were dispersed with different amount of sodium dodecylbenzenesulfonate (SDBS) prior to the PEI functionalization. The resulting samples exhibit air-stable n-type characteristics with electrical conductivities as great as 1500 S/m and thermopowers as large as -100 μV/K. Electrical conductivity and thermopower were strongly affected by CNT dispersion, improving the properties with better dispersion with high concentrations of SDBS. This improvement is believed to be due to the increase in the number of tubes that are evenly coated with PEI in a better dispersed sample. Increasing the amount of PEI relative to the other constituents positively affects thermopower but not conductivity. Air exposure reduces both thermopower and conductivity presumably due to oxygen doping (which makes CNTs p-type), but stable values were reached within seven days following sample fabrication.

*Parts of this section are reprinted from "N-type thermoelectric performance of functionalized carbon nanotube-filled polymer composites," by D. Freeman, K. Choi, and C. Yu, PLos One, 7, e47822 (2012) with permission by PLos One.

5.2 Experimental

Carbon nanotubes, made using chemical vapor deposition by CheapTubes Inc., were used for the experiment. The manufacturer claimed the 90 wt% purity CNTs contain single wall nanotubes whose specifications are the following: outer diameter: 1-2 nm, inner diameter: 0.8-1.6 nm, length: 5-30 μm, ash: < 1.5 wt%, multi-wall nanotubes: > 5 wt%, amorphous carbon: < 3 wt%. The 99 wt% purity CNTs contain approximately 50/50 single- and double-wall tubes whose specifications are the following: outer diameter: 1-2 nm , inner diameter: 0.8-1.6 nm, length: 3-30 μm, ash: 0 wt%, multi-wall nanotubes: < 2 wt%. For each experiment, 60 mg of CNTs were dispersed in 5~15 ml of deionized water with a prescribed amount of SDBS. Sonication was conducted in two modes. The mixture was sonicated for 30 min using pen-type sonicators (XL-2000 from Misonix and FB 120 from Fisher scientific). Afterward, a determined amount of aqueous 5-wt% PEI (branched, M.W. 600, 99% from Alfar Aesar) solution was added with a pipette into the dispersion. It has been demonstrated that PEI attaches to nanotubes by physisorption on the tube sidewall [42]. To maximize the occurrence of physisorption and create an even coating of PEI on the nanotubes, the mixture solution was stirred for 48 hours while being maintained at a temperature of 50-60 °C. The prescribed amount of PVAc (Vinnapas 401, Wacker chemicals) was subsequently added into the dispersion. The mixture was dispersed by pen-type sonicators for 30 minutes each and then poured into a 5 cm × 5 cm × 2 cm plastic container for casting. Films of 20-80 μm in thickness were formed as the dispersion dried, in a process that usually took between 24 and 48

hours. Dried samples were then thermally annealed in a vacuum oven at 60° C for 4 hrs in order to remove any water which had permeated the film.

After fabrication, each sample was tested for conductivity and thermopower values. To this end, a rectangular test sample of the dried and annealed film was removed from the plastic container. Conductive silver paint was applied to the sample strip to minimize electrical contact resistance and the relevant dimensions were measured using a micrometer. Details can be found in previous sections.

5.3 Results and discussion

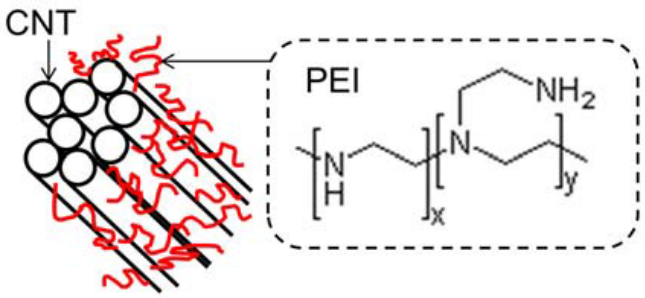

Figure 13. Schematic representation of PEI-functionalized CNT bundles in the composites and the structure of branched PEI. The amine groups are responsible for the electron donation which converts CNTs into n-type semiconductors. When the bundles are smaller, more tubes come in direct contact with PEI, which increases the n-type thermopower values. On the other hand, composites with large bundles have fewer junctions necessary for electron transport across the composite (reprinted from [103]).

The PEI used in this study had an average molecular weight of ~600, indicating that it was composed of molecules that were made of four to five units like the one shown in Figure 13. Although covalent bonding has been demonstrated for the case of

Ffunctionalized (fluorinated) CNTs, pristine CNTs like those used in this study interact with PEI dominantly via physisorption [104, 105] rather than chemisorption. In this process, the PEI molecules wrap around the CNTs and form bonds with other PEI molecules or with the opposite ends of the same molecule. It has been shown with atomic force microscope imaging that this coating of PEI molecules causes the tube to double in diameter relative to uncoated tubes [106]. In our experiments, when tubes were soaked in PEI solutions, and then filtered, rinsed, and allowed to dry, the product was heavier than the tubes prior to the process. In addition to adding mass, PEI also acts as a coagulant for CNTs in water which can counteract the effects of the surfactant. Visible tube agglomerations were observed when the ratio of PEI wt% to CNT wt% is higher than 0.5 during the PEI doping process. Such aggregation often makes the sample mechanically weak and/or hinders composite formation.

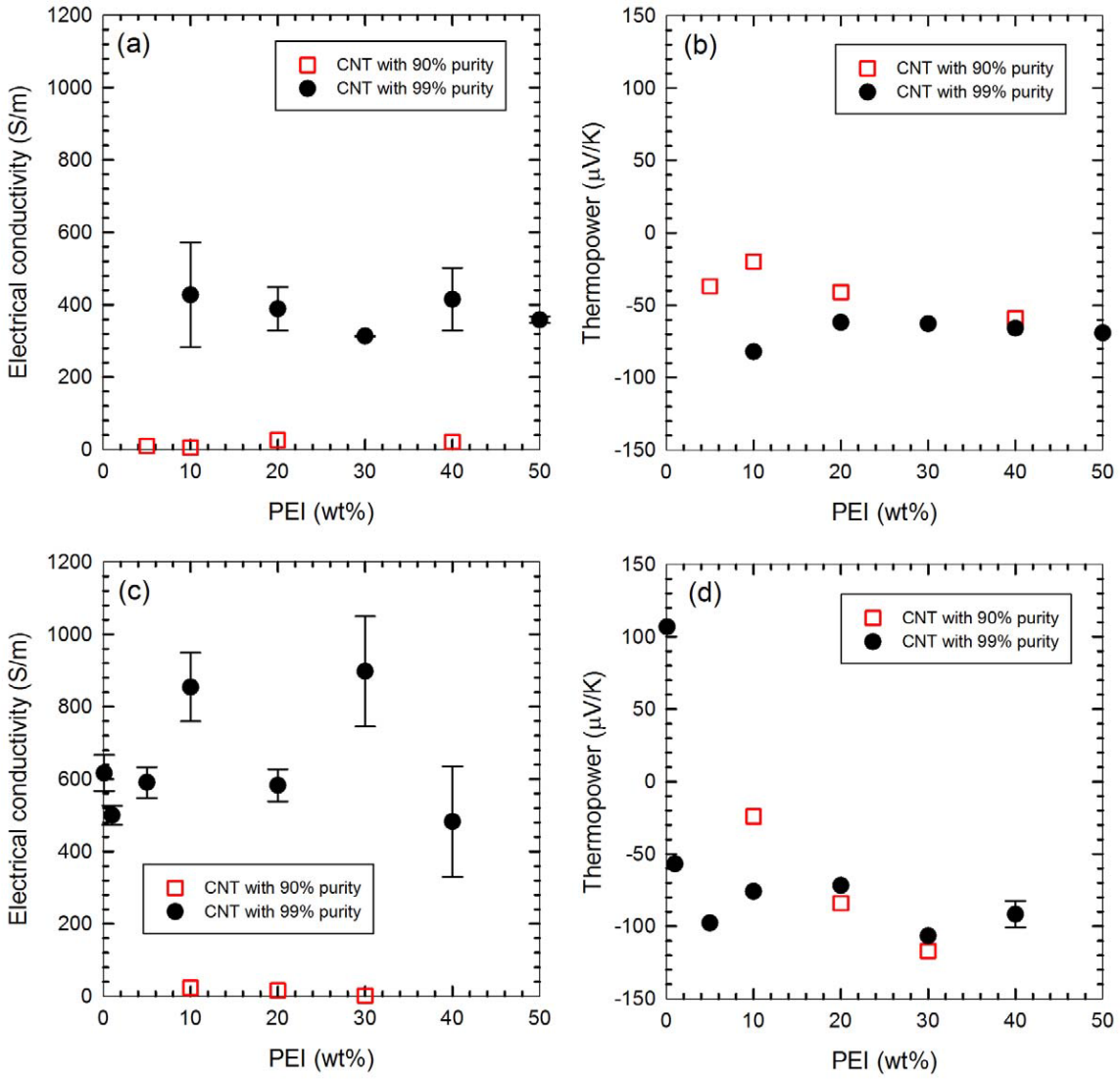

Figure 14. Effect of PEI wt% on the electrical properties for the samples containing 20 wt% (a and b: Series 1) and 40 wt% (c and d: Series 2) SDBS (reprinted from [103]).

Series 1 and Series 2 varied the amount of PEI, being composed of 20-wt% CNT with 20-wt% (for Series 1) or 40-wt% (for Series 2) SDBS. When the higher SDBS concentration was used, electrical conductivity was more or less improved, presumably due to the better CNT dispersion. The data are somewhat scattered but the overall values

for electrical conductivity are higher for the 40-wt% SDBS samples, compared to the 20 wt% samples. The change in thermopower values is rather small due to the small absolute values as well as the weighting factor (electrical conductivity) for n- and p-type thermopower of CNTs in the composite materials. The composites contain less SDBS compared to the best properties in Series 1 (60-wt% SDBS). As we had more CNTs compared to SDBS, it is much harder to disperse CNTs, which is a part of the reasons for the scattered properties. It should be noted that, unlike p-type properties, n-type strongly depends on PEI coverages. On the other hand, the samples exhibited little change with increasing PEI beyond 10 wt%, possibly indicating saturation (Figure 14). Beyond this point, it is likely that no rooms are available for additional PEI to attach.

The first three levels of Series 2 (0.1, 1, and 5-wt% PEI, in Figure 14(d)) demonstrate a correlation between PEI weight percent and thermopower. The sample containing only 0.1 wt% has a p-type thermopower comparable to control samples made without incorporating PEI. The 1-wt% sample exhibits n-type properties of a lower magnitude. Above 5 wt%, the samples demonstrate only a slight correlation with thermopower and additional PEI weight percent. Doping fractions by nitrogen per each carbon in CNTs were estimated. Assuming the structure of the branched PEI is shown in Figure 13 with x and y are 1 (i.e., 1 unit contains 3 nitrogen). Then, molecular weight of 5 units is ~645, which is close to the specification from the manufacturer. The n-type conversion occurred when the ratio of CNT to PEI wt% is 1:0.05 (i.e., 1 wt% PEI sample). In this case, the number of nitrogen per carbon can be calculated to be $\sim 3 \times 10^{-3}$. In fact, this value is within the range, $1 \sim 6 \times 10^{-3}$ [51] suggested by an experiment

with a field-effect transistor configuration made of PEI-functionalized CNT. This may explain that relatively constant thermopower when PEI is more than 10 wt%.

5.4 Conclusions

In the future, studies could be conducted to optimize n-type doping along with p-type doping [6, 26] by adjusting the ratios between CNT, SDBS, PEI, and other molecules or chemicals. Oxygen barriers could be used to prevent degradation of n-type properties. Eventually, working combined p- and n-type modules can be fabricated and evaluated for the thermoelectric figure of merit [23]. This work will pave the way for lightweight, non-toxic and flexible thermoelectric cells capable of harvesting thermal energy from the human body, solar cells and a host of other areas where it is currently going to waste as well as cooling energy consuming devices.

CHAPTER VI

MANIPULATING THERMOELECTRIC BEHAVIOR OF CNT/PEDOT:TOS HYBRIDS FOR LARGE THERMOPOWER

6.1 Introduction

The electrical properties of polymer based thermoelectric material can be manipulated by n- or p-type doping by organic or inorganic materials. Due to its low thermal conductivity, it is attractive to use it as thermoelectric applications if it is possible to enhance the electrical properties while suppressing the thermal conductivity. One of the promising conductive polymer is poly(3,4-ethylenedioxythiophene) (PEDOT) since it has high electrical conductivity (~10^4 S/m when doped with dimethylesulfoxid (DMSO)) and low thermal conductivity (~0.2 W/m-K at room temperature). However, relatively low thermopower compared to inorganic materials such as Bi-Te alloys impede PEDOT as a good candidate of thermoelectric applications. In this research, tosylate (Tos) anions will be attached to the PEDOT molecules to make PEDOT-Tos polymer. By reduction of tetrakis (dimethylamino) ethylene (TDAE) in an inert environment, electrons will be depleted from TDAE to PEDOT-Tos molecules (Figure 15), resulting in n-type doping of the polymer chains. The electrical conductivity and the thermopower will be decreased and increased, respectively, due to less hole carriers in PEDOT-Tos. The electrical conductivity and thermopower can be manipulated by

reduction level of tetrakis, and be optimized for maximum power factor. The maximum thermopower was obtained as ~800μV/K with 10^{-2} S/m of electrical conductivity by Bubnova et al [107] with similar method.

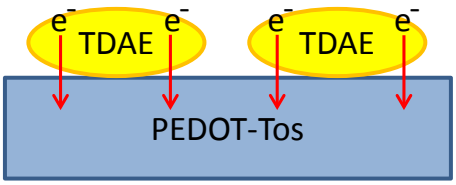

Figure 15. Vaporized TDAE molecules are attached on the surface of the PEDOT-Tos film. The electrons will transfer from TDAE molecules to PEDOT-Tos chains, resulting in n-type doping of PEDOT-Tos film.

6.2 Experimental

2mg of single walled carbon nanotubes (a purified grade called P2, synthesized by arc discharge method from Carbon Solutions Inc.) were dispersed in 20ml of deionized (DI) water with 6mg of sodium dodecyl benzene sulfonate (SDBS, Acros organics, 88%) with 24 hours of ultrasonication. Then, the supernatant solution was obtained after 20min of centrifuge at 12000 rpm in order to have well de-bundled nanotubes without impurities. According to the manufacturer, P2-SWNT includes 4 to 7 wt% of Ni and Y, and carbonaceous purity greater than 90 wt%. The average diameters of the individual and bundled tubes are 1.5 and 4-5nm, respectively. The length of the nanotubes ranges from 500nm to 1.5μm. Above solution was sprayed on a quartz slide at ~80^{o}C of surface temperature with an airbrush (Fuso Seiki Co., GP-S1, 0.2mm nozzle diameter) for different spraying time in order to obtain dissimilar nanotube networks.

The samples were then carefully immersed into DI water for 15min to remove SDBS and dried afterward. EDOT polymerization with iron tosylate was referred to other's work [Nature Materials]. 50μl of 3,4-ethylenedioxythiophene (TCI, 98+%), 1ml of diluted iron (III) tris-p-toluenesulphonate in n-buntanol (Clevios^{TM} C-B 40 V2, solid contents of 38-42%), and 1ml of n-Butanol (EMD) were mixed with Pyridine (Alfa Aesar, 99+%)(0.5 mol per 1mol of iron tosylate) in order to control the kinetics of the polymerization. Prepared solution was spin-coated on above nanotube sprayed quartz substrates at 2000 rpm for 35s. The average sample thickness was obtained from 60-90nm by Veeco optical profilometer. Multiple measurements were performed since the electrical conductivity analysis is remarkably sensitive to the thickness of the samples. Subsequently, the samples were placed in a convection oven at 110^{o}C for 10min to be polymerized, and then naturally cooled to room temperature for ~30min. Finally, the samples were immersed into DI water to remove residual Fe (III) tosylate for 10min and dried.

For reduction of the samples, few drops of tetrakis (dimethylamino) ethylene (TDAE) (Sigma Aldrich, 85+%) were widely spread on the bottom of the common plastic box, and prepared sample was attached on the lid of the box with coated side down. PEDOT-Tos was reduced under low level of vacuum (9 inHg) with 25% of relative humidity at room temperature. The electrical properties of PEDOT-Tos/CNT hybrid were controlled by varying TDAE exposure time for different reduction status.

6.3 Results and discussion

Table 3. Sample list with different CNT spraying time and reduction level.

Sample number	Spraying time	Reduction time
1-1	5sec	0min
1-2		10min
1-3		30min
1-4		60min
2-1	15sec	0min
2-2		10min
2-3		30min
2-4		60min
2-5		90min
3-1	30sec	0min
3-2		10min
3-3		30min
3-4		60min
3-5		90min
4-1	45sec	0min
4-2		10min
4-3		30min
4-4		60min
5-1	90sec	0min
5-2		10min
5-3		30min
5-4		60min

In order to study the influence of reduction levels in different concentrations of CNTs, 5, 15, 30, 45, and 90sec of CNT sprayed samples were exposed to tetrakis vapor from 0 to 60min (Table 3). In Figure 16, simple schematic of the process of PEDOT-Tos preparation is shown. PEDOT-Tos films can be synthesized by simple spin coating and

reduction process. Few drops of prepared PEDOT-Tos solution will be placed on the glass slide. The solution can be spin coated at different rpms, in order to control the reduction level further. The resulting samples will be annealed at 110^{o}C for 5 min on a hot plate in order to polymerize the PEDOT-Tos film. After finishing the polymerization, residual iron tosylates were removed by washing with deionized water. Few drops of TDAE were placed in a closed chamber with PEDOT-Tos sample, and then proper vacuum level will be applied for TDAE vapor reduction. The reduction level can be controlled by different reduction time of the resulting PEDOT-Tos films.

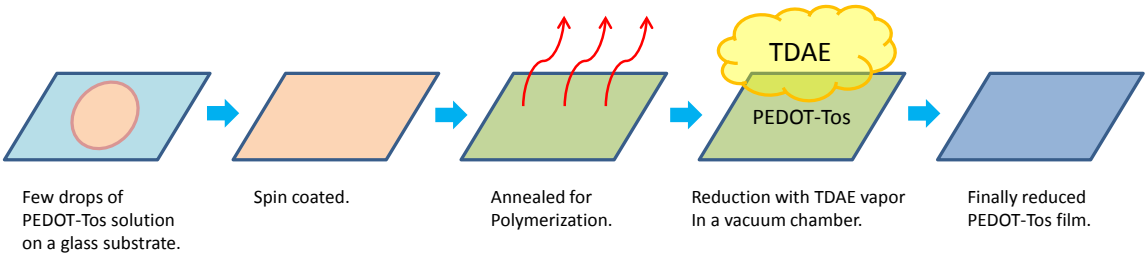

Figure 16. PEDOT-Tos preparation process. The PEDOT-Tos film can be simply spin coated on a glass slide, and reduced with vaporized TDAE molecules.

In order to enhance the electrical conductivity without sacrificing thermopower, carbon nanotubes (CNTs) was be added into PEDOT-Tos film as conductive filler. The concentration of the CNT need to be controlled because the electrical properties of the CNT/PEDOT-Tos film will follow those of CNTs if the CNTs form networks in the matrix. In case of lower CNT concentration than its percolation threshold, it will be evenly distributed in the PEDOT-Tos matrix, constituting local channels for carrier transport (Figure 17). The concentration of the fillers will be changed from 0.0005wt%

to little higher than its percolation threshold for optimize the power factor with high thermopower. Disconnected channels will filter lower energy carriers, resulting in higher thermopower from elevated average energy of total carriers. Different types of fillers, such as single, double, and muti-walled CNTs can be incorporated for investigate the influence of different types of carrier channels. The intrinsic electrical and thermal properties, geometrical factors will alter the thermoelectric properties of the samples.

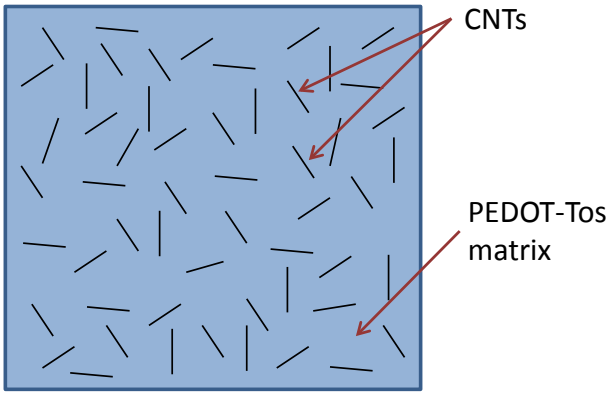

Figure 17. Low concentration of CNTs is evenly distributed in a PEDOT-Tos film, resulting in disconnected local electron channels.

First, CNT network structure was investigated. The concentration of the CNTs was controlled by different spraying time and the network structures were inspected under scanning electron microscope, as shown in Figure 18. In order to verify the effect of nanotube network, nanotubes were well dispersed in aqueous solution, and spraying was precisely controlled. A few nanotubes were dispersed on substrate at short spraying time (5sec and 15sec), but the network was totally percolated at 45 sec of spraying. The particles shown in the images are thought as to be SDBS.

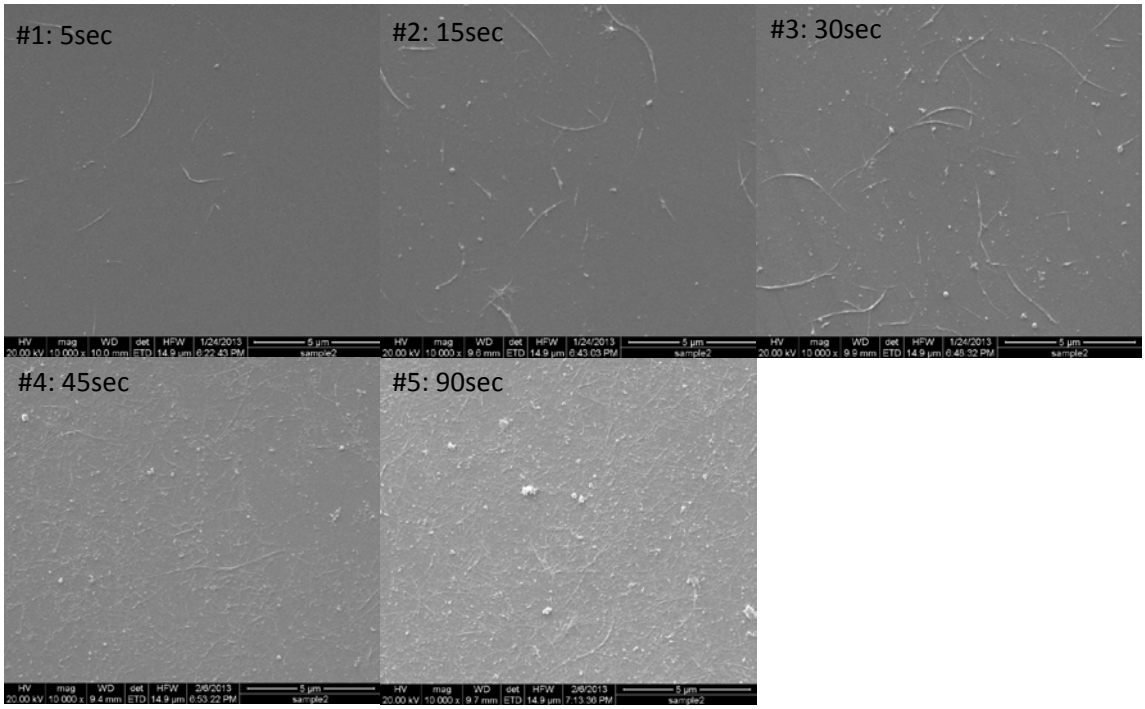

Figure 18. Scanning electron micrographs of the surface of substrate right after CNT spraying. Denser nanotube network was achieved as increasing spraying time. It is seemed that the network was percolated at 45 sec of spraying. All scale bar included are 5μm.

Thermoelectric behaviors were measured with a function of reduction time. The electrical conductivity of the CNT/PEDOT-Tos hybrids was ~6,000 to ~11,000 S/m without reduction. However, the electrical conductivity of the all samples was suddenly decreased even though the samples were exposed to tetrakis vapor only for 10 min (Figure 19(a)). As increasing reduction time, we could not find noticeable change in electrical conductivity. The conductivity of 90 sec and 45 sec spraying samples showed much higher values through whole range of reduction time since the major electron transport pathway was percolated nanotube networks rather than polymer matrix. In Figure 19(b), dramatic increase of thermopower was observed as increasing exposure

time to tetrakis. Generally, the thermopower of each sample was increased by 30min of reduction, and then saturated. The thermopower of the sets, rated from highest to lowest, were 15sec, 30sec, 5sec, 90sec and 45sec. The maximum thermopower was obtained as ~11mV/K at 15 sec of spraying sample with 30min of reduction.

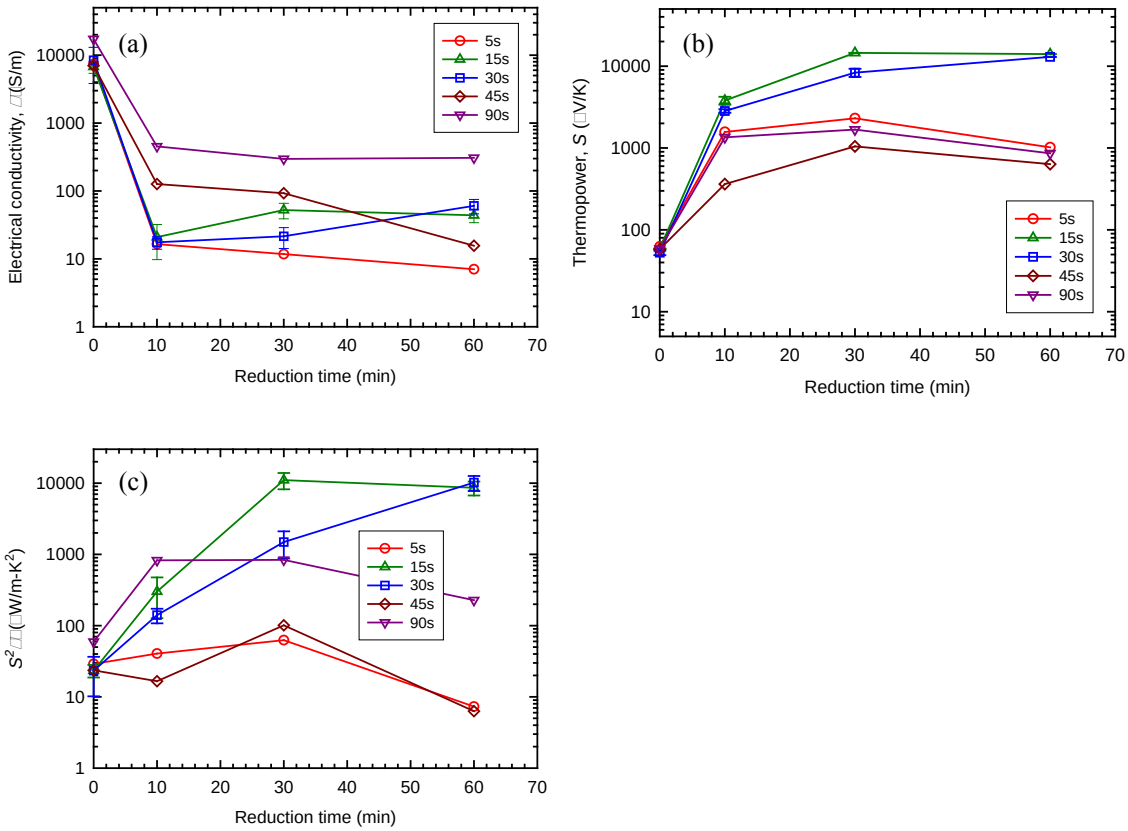

Figure 19. Electrical conductivity (a), thermopower (b), and power factor (c) of sample CNT/PEDOT-Tos hybrid samples. All the conditions were fixed except CNT solution spraying time. The reduction effect was saturated at 30 min of exposure to tetrakis vapor.

This is more than one order magnitude higher than any other reported values among organic thermoelectric materials. From this result, it would be explained that nanotube network and reduction level are important factors to manipulate thermopower. The optimized nanotube concentration for thermopower was 15 sec, which was lower than percolation threshold. 30sec of spraying sample also showed slightly lower thermopower (~10mV/K), but these values are much higher than that of 5 sec, 45 sec, or 90 sec spraying samples.

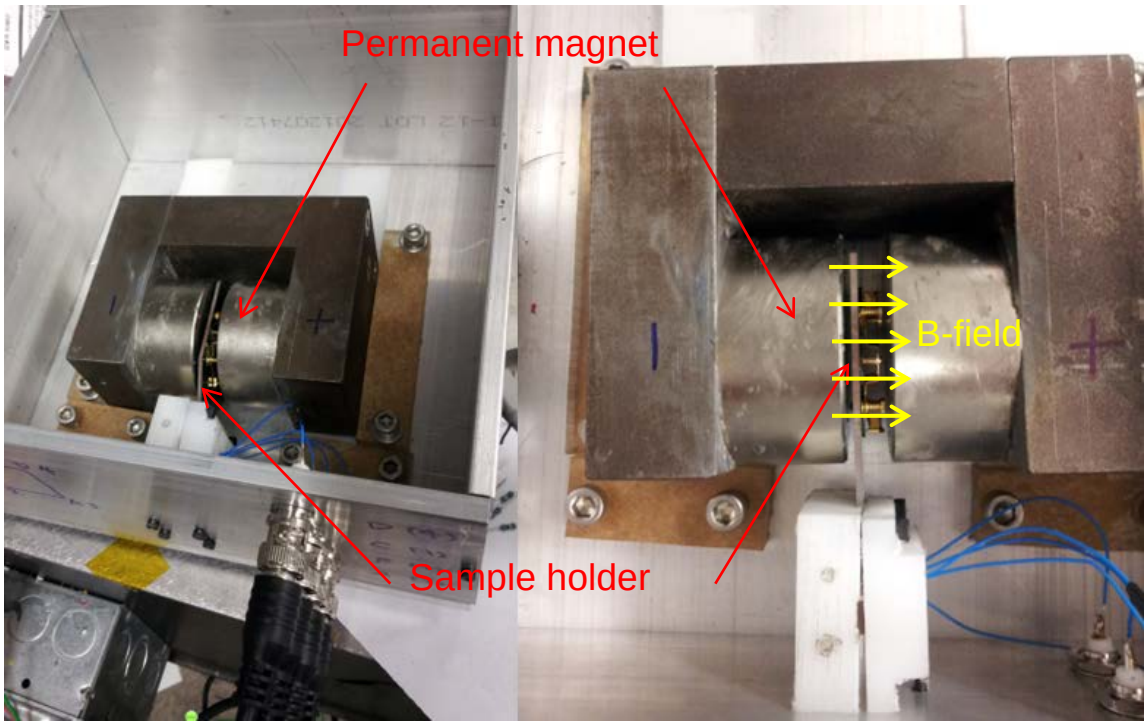

Figure 20. Hall measurement apparatus with 1T of permanent magnet and sample holder

In order to study the n-type doping effect as increasing reduction time, hole carrier concentration and mobility were measured by home-made Hall test apparatus (Figure 20). Since the optimized results were obtained with 15sec spraying samples, 0 to 60min of reduced samples were prepared for Hall test. Samples were coated on polycarbonate substrate, and cut into 1cm by 1cm of square shape. Silver paint was applied on the four corners of the sample, in order to make a better electrical contact between sample and electrodes. After mount the sample, 1T of magnetic field was applied with certain amount of current into the sample. Then, the hole carriers in the sample would move to one side by the Hall effect. From the migration of the carriers, induced Hall voltage was recorded by Keithley multimeter as a function of time. At least 100 points were recorded and then averaged to get the Hall voltage for each configuration (Figure 21). By measuring sheet resistance and Hall voltages, the carrier concentration and mobility of each sample were possible to obtain.

Hole carrier concentration and mobility behavior as reduction level was illustrated in Figure 22. Without reduction, carrier concentration was around 10^{21} /cm^3, which was similar to typical conductive polymers. However, the concentration was suddenly dropped to 10^{18} /cm^3 after reduction, and then almost saturated at 30 to 60min of reduction. This is direct evidence of n-type doping of PEDOT, since the number of hole in the sample was reduced by heavy injection of electrons as increasing reduction time. Hole mobility was initially ~1cm^2/Vs, which was close to literature values for conductive polymers. After reduction, the mobility was dramatically increased to ~14cm^2/Vs, and saturated. Such kind of high mobility could be a probable reason for the

outstanding thermopower of reduced samples. Non percolated CNT networks increased hole mobility by local pathways, and achieve elevated energy levels of carriers resulting high thermopower.

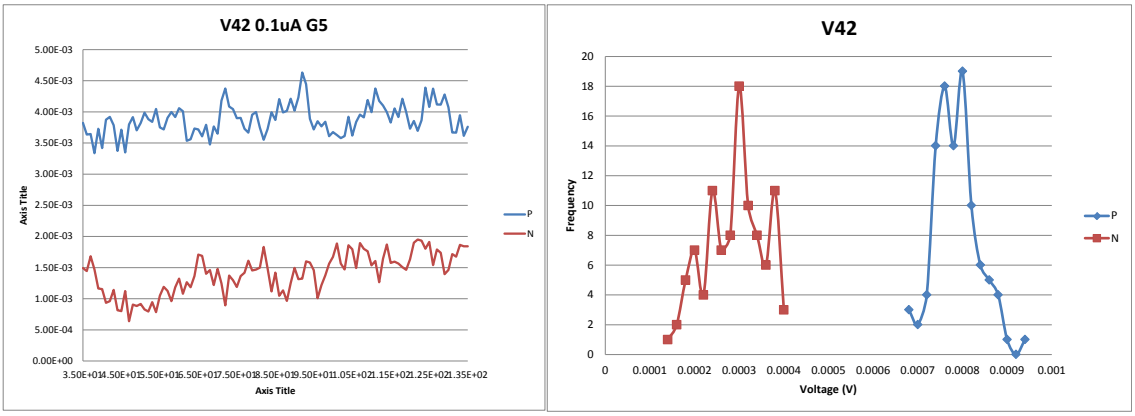

Figure 21. A representative Hall voltage signal from Keithley multimeter. Two different voltages were obtained by different polarity of the magnet (P and N). Right hand side graphs are re-organization with histograms.

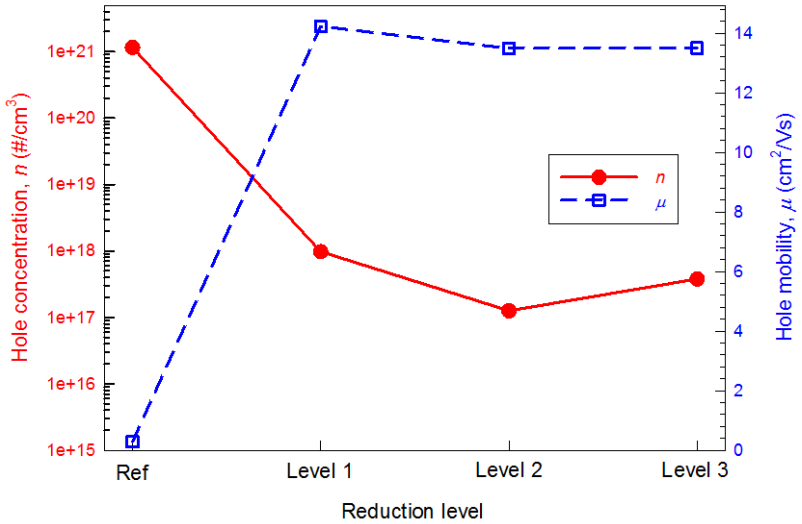

Figure 22. Hole concentration and mobility were obtained by Hall measurement method. The concentration and is reduced and saturated at ~10^{18} /cm^3, and very high mobility was obtained after reduction.

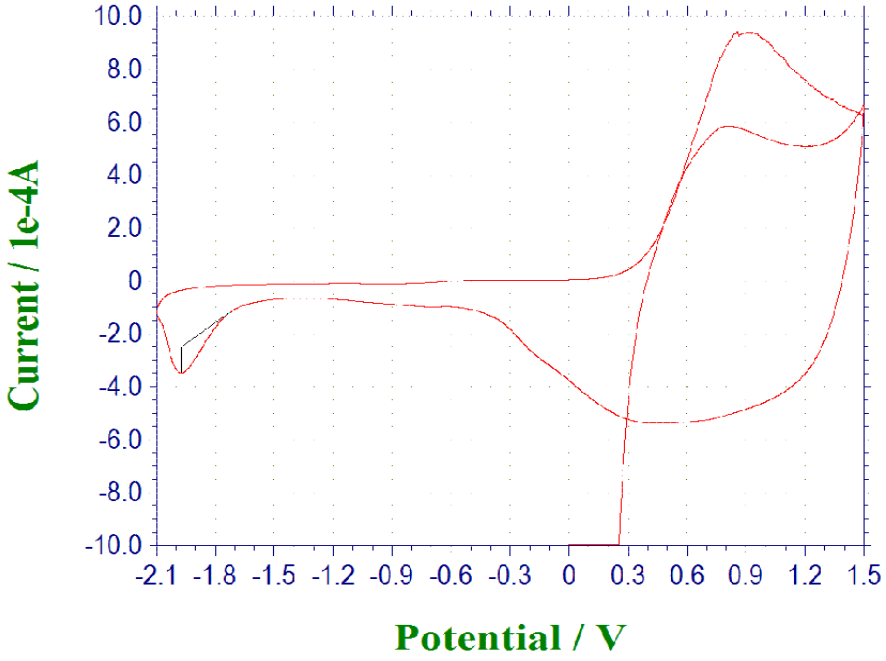

Figure 23. CV data of CNT 15sec sprayed/PEDOT-Tos sample with 60min of reduction. The oxidation and reduction onset was found as 0.1 and -1.4V respectively, resulting 4.9eV of HOMO and 3.4 of LUMO.

In order to verify n-type doping effect on PEDOT, electronic band gap structure was analyzed. In conductive polymers, conduction band and valence band can be replaced with LUMO (Lowest Unoccupied Molecular Orbital) and HOMO (Highest Occupied Molecular Orbital), respectively. LUMO, HOMO and band gap were obtained by cyclic voltammetry (CV) analysis for 15sec CNT sprayed with PEDOT-Tos sample set. One of representative CV is shown in Figure 23, based on the oxidation and reduction onset potentials using ferrocene and external standard. A glassy carbon electrode was used as a working electrode, a Pt wire was used as a counter electrode, and an Ag/Ag^{+} electrode was used as a reference electrode in 0.01-M $AgNO_3$ in acetonitrile. The half-wave potential of Fc/Fc+ redox couple ($E_{1/2}(F_c/F_c^{+})$) was estimated from (E_{ox} +

E_{red})/2, where E_{ox} and E_{red} are the oxidation and reduxtion peak potentials, respectively. $E_{1/2}(F_cF_c^+)$ was found to be -0.04V relative to the Ag/Ag^+ reference electrode. From this, HOMO and LUMO (eV) were calculated by using the following equation.

$$\text{HOMO (or LUMO)} = -4.8+E_{1/2}(F_c/F_c^+)-(\text{Oxidation or Reduction onset}) \quad (10)$$

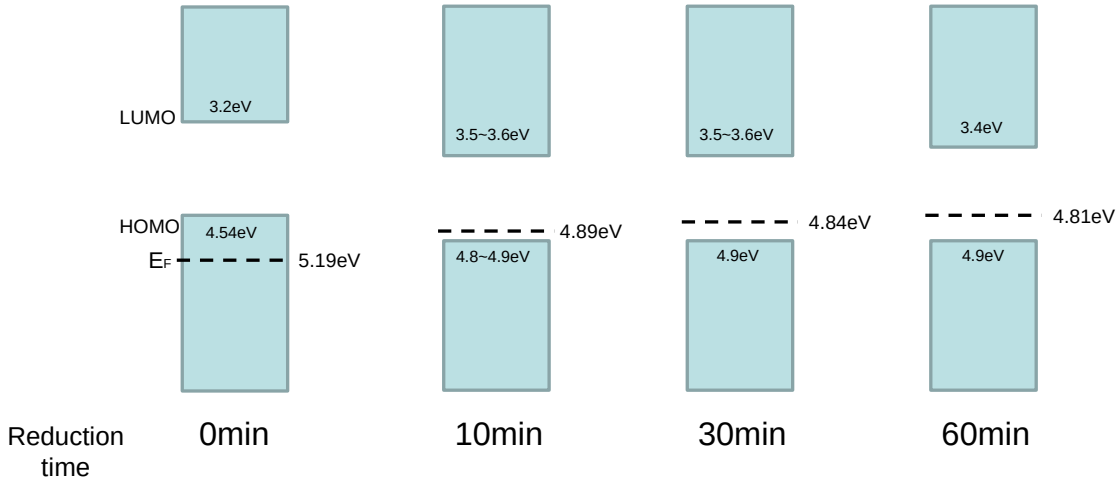

Figure 24. Electronic band gap structure of CNT 15sec sprayed/PEDOT-Tos sample set (0 ~ 60min of reduction). Larger band gap and up-shifted WF were observed compared to reference (0min) sample.

The location of Fermi energy level was determined by contact potential difference (CPD) method, which is the work function (WF) difference between a probe and sample, was measured by Kelvin probe method in air environment. Since the WF of a probe tip may be affected by moisture and other contaminants in air, the CPD of gold foil was measured for calibration and was found to be -150mV. If the Fermi level of the gold foil would be assumed as -5.10eV, that of sample set can be calculated. According

to both analyses, it was possible to get HOMO, LUMO, and WF of the samples so as to complete the electronic band gap structures (Figure 24).

Based on the full band gap information above, direct evidence of n-type doping effects was revealed. First, the initial band gap without reduction was found as ~1.34eV. After reduction, the band gap was suddenly enlarged to ~ 1.4 to 1.5eV, which might be a reason of band gap shinkage due to electron injection. For semiconductors, the WF of p-type semiconductors is located near valence band (HOMO), and that of n-type material is located near conduction band (LUMO). The WF of reference sample (0min) was calculated as 5.19eV, which was closed to HOMO. However, it was up-shifted after reduction (4.89eV), and then slightly and continuously moves toward to LUMO level (4.81eV) as increasing reduction time. This is due to more electron injection to hole-rich PEDOT-Tos.

6.4 Conclusions

Polymer composites containing low concentration of CNT were prepared. The volume % was controlled with spraying time, and then estimated with SEM images. Non-percolated CNT network was effective to enhance the electrical conductivity as well as thermopower, since the hole carrier concentration and mobility were increased by local pathways of CNTs. If the CNTs are percolated, electrical conductivity was increased to few hundreds of S/m even though after vigorous reduction, but the thermopower was inferior to non-percolated samples because the electrical contribution

of CNT is dominant rather than PEDOT matrix. In order to verify the outstanding thermopowers, Hall test were performed to obtain carrier concentration and mobility. The entire electronic band gap structure was completed by CV and CPD method, and then revealed the direct evidence of n-type doping of samples by confirming enlarged band gap and up-shifted work function in reduced samples.

CHAPTER VII

CONCLUSION AND FUTURE WORK

7.1 Improved thermoelectric behavior of organic nanocomposites with conductive stabilizer

The thermoelectric properties of carbon nanotube (CNT)-filled polymer composites can be enhanced by modifying junctions between CNTs using poly(3,4-ethylenedioxythiophene) poly(styrenesulfonate) (PEDOT:PSS), yielding high electrical conductivities (up to~40000 S/m) without significantly altering thermopower (or Seebeck coefficient). This is because PEDOT:PSS particles are decorated on the surface of CNTs, electrically connecting junctions between CNTs. On the other hand, thermal transport remains comparable to typical polymeric materials due to the dissimilar bonding and vibrational spectra between CNT and PEDOT:PSS. This behavior is very different from that of typical semiconductors whose thermoelectric properties are strongly correlated. The decoupled thermoelectric properties, which is ideal for developing better thermoelectric materials, are believed to be due to thermally disconnected and electrically connected contact junctions between CNTs. Carrier transport at the junction is found to be strongly dependent on the type and concentration of stabilizers.

7.2 Large Thermoelectric figure of merit for flexible and light-weight organic composites with carbon nanotubes

Typical organic materials have low thermal conductivities that are best suited to thermoelectrics, but their poor electrical properties with strong adverse correlations have prevented them from being feasible candidates. The composites in this study, containing single-wall carbon nanotubes, poly(3,4-ethylenedioxythiophene):poly(styrenesulfonate) and/or polyvinyl acetate, show thermopowers weakly correlated with electrical conductivities, resulting in large thermoelectric power factors in the in-plane direction of the composites,~160 $\mu W/m\text{-}K^2$ at room temperature, which are orders of magnitude larger than those of typical polymer composites. Furthermore, their high electrical conductivities, $\sim 10^5$ S/m at room temperature, make our composites very promising for various electronic applications. The optimum nanotube concentrations for better power factors were identified to be 60 wt % with 40 wt % polymers. It was noticed that high nanotube concentrations above 60 wt % decreased the electrical conductivity of the composites due to less effective nanotube dispersions. The thermal conductivities of our 60 wt % nanotube composites in the out-of-plane direction were measured to be 0.2 ~ 0.4 W/m-K at room temperature. The in-plane thermal conductivity and thermal contact conductance between nanotubes were also theoretically estimated.

7.3 Highly doped carbon nanotubes with gold nanoparticles and their influence on electrical conductivity and thermopower

Various kinds of CNTs were imbedded in polymer matrix with p-type doping by gold nanoparticles. The concentration of CNT was fixed, and that of gold was varying from 0 to 20 vol% in order to verify the effect of p-type doping of gold. The electrical conductivity of p-doped composite was maximized to ~6×10^5 S/m by replacing 15-vol% PEDOT:PSS with gold nanoparticles. This result is orders of magnitude higher than those of other polymer composites with same concentration of CNTs. A variable range hopping model with a parallel resistance model was applied to investigate the effect of gold nanoparticles in p-type doping. Moreover, different types of CNTs were tested with same recipe of the optimized one so as to see the resulted electrical conductivity of the samples are dominated by intrinsic property of CNTs.

7.4 N-type thermoelectric performance of functionalized carbon nanotube-filled polymer composites

CNTs were combined with polymers to synthesize composites, and their electrical and thermal properties have been evaluated. Despite typical correlation between thermal and electrical conductivities, these composites exhibit electrical conductivities nearly as high as films composed exclusively of tubes, but still possess thermal conductivities closer to those their polymer matrices. This phenomenon results from the relative ease with which charge carriers travel across the nanotube networks by hopping. The thermal carriers, or phonons, have relative difficulty with transport because they are scattered at the CNT surfaces and at the junctions between the tubes. The result is a material with high electrical conductivity and low thermal conductivity. For example, composites p-type doped CNTs exhibited electrical conductivities as high as ~10^5 S/m. While several studies have been conducted on carbon nanotube/polymer composites, none of them have investigated the thermoelectric properties of such polymers when the nanotubes are converted into air-stable n-type. The overall aim of this study was to produce and test such composites and to determine the conditions which result in the best thermoelectric performance.

7.5 Manipulating thermoelectric behavior of CNT/PEDOT-Tos hybrids for large thermopower

Thermoelectric properties of PEDOT-Tos were enhanced with CNT networks. By controlling of CNT concentration and reduction level, it was possible to achieve ~10,000 μV/K of outstanding thermopower with ~100 S/m of electrical conductivity. Large thermopower was achievable since the local pathways of CNT increased carrier mobility and average energy of carriers. Carrier concentration and mobility were measured by home-made Hall test apparatus, and HOMO, LUMO, and work function were measured by CV and CPD method. From the full electronic band gap structure, it was possible to explain the n-type doping effect by enlarged band gap and up-shifted Fermi level of reduce samples.

7.6 Future work

There are numerous avenues for additional research in organic thermoelectric materials with CNTs. Among those, two areas are described in more detail below, including thermal conductivity analysis of the CNT/polymer composite and p- and n-junction of CNT/PEDOT-Tos legs for thermoelectric module.

7.6.1 *Thermal conductivity analysis of the CNT/polymer composite*

In order to have full analysis on thermoelectric properties, it is necessary to have the information of thermal conductivity of the material. However, thermal conductivity measurement in in-plane direction is relatively hard compare to out-of-plane direction.

For isotropic materials, it is not necessary to measure both directions, but high concentration of fillers such as CNTs in polymer matrix results high anisotropy in the network structure.

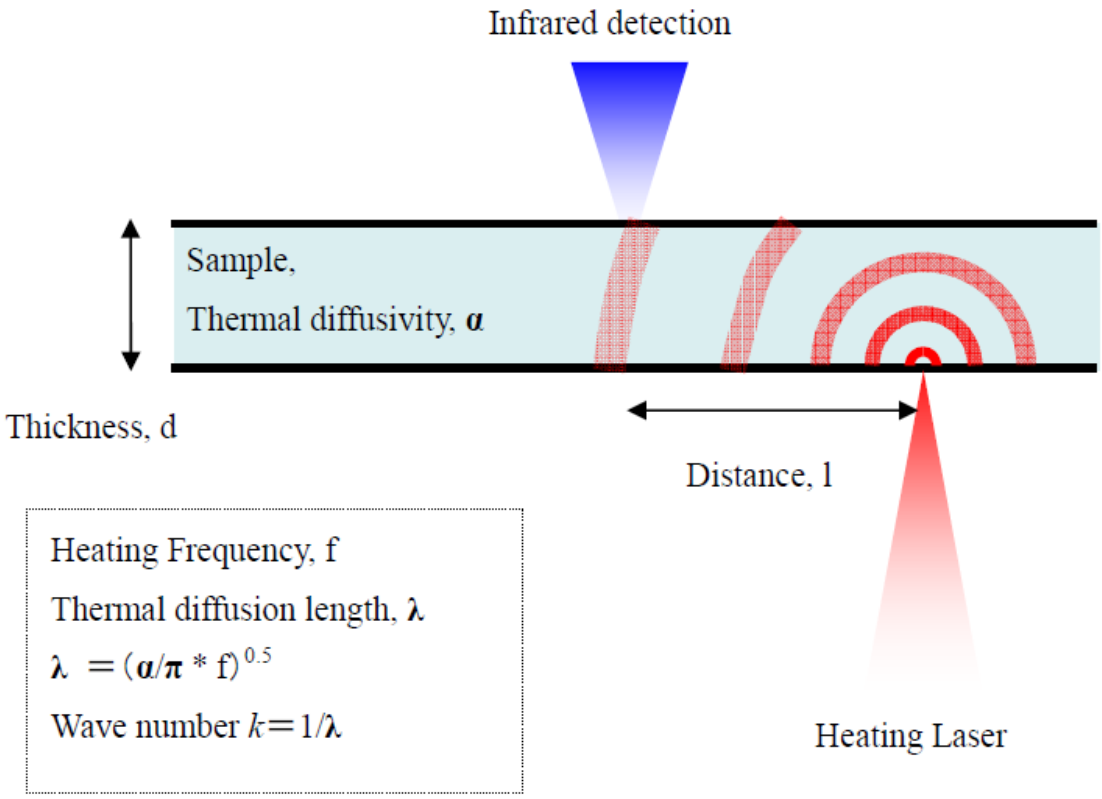

Figure 25. A schematic of thermowave technique for in-plane diffusivity measurement.

A thermowave technique would be a promising candidate for in-plane thermal conductivity measurement in thin films. As shown in Figure 25, modulated heating laser induces propagation of thermal signal. It is possible to obtain the in-plane thermal diffusivity by phase lag of the sinusoidal heat pulse from the source. If this is viable, it would be possible to get the ZT values of the thin films and reveal the correlation between in- and out-of-plane thermal conductivities with CNT concentrations.

7.6.2 *p- and n-junction of CNT/PEDOT hybrids*

From the result of Chapter VI, it seems possible to change the electric property of PEDOT from p-type to n-type by doping process. If there is a proper and stronger electron donor to PEDOT, it would be possible to get n-type CNT/PEDOT hybrid. Since the PEDOT can be dissolved in proper solvent, it would be viable to print PEDOT on a substrate.

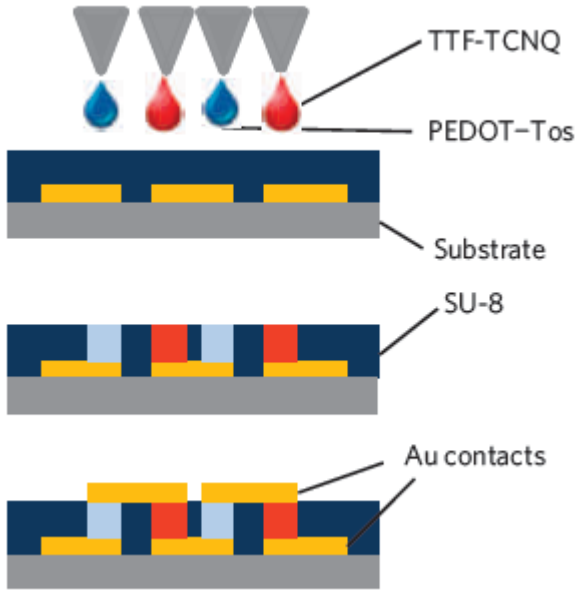

Figure 26. Organic p- and n- junction for thermoelectric power generation module [107].

Bubnova et al. suggested the printing method with organic materials in Figure 26. They used TTF-TCNQ as an n-type material, but the thermopower is too low (~28μV/K) compared to p-type CNT/PEDOT-Tos hybrid (~10,000 μV/K). Absolutely, the power output would be enhanced if the thermopower of n-type PEDOT material is few hundreds to thousands of μV/K.

REFERENCES

1. Majumdar, A., *Thermoelectricity in semiconductor nanostructures.* Science, 2004. **303**(5659): p. 777-778.
2. Harman, T.C., et al., *Quantum dot superlattice thermoelectric materials and devices.* Science, 2002. **297**(5590): p. 2229-2232.
3. Venkatasubramanian, R., et al., *Thin-film thermoelectric devices with high room-temperature figures of merit.* Nature, 2001. **413**(6856): p. 597-602.
4. Hsu, K.F., et al., *Cubic AgPbmSbTe2+m: Bulk thermoelectric materials with high figure of merit.* Science, 2004. **303**(5659): p. 818-821.
5. Hu, M., D.M. Yu, and J.B. Wei, *Thermal conductivity determination of small polymer samples by differential scanning calorimetry.* Polymer Testing, 2007. **26**(3): p. 333-337.
6. Grunlan, J.C., et al., *Thermal and mechanical behavior of carbon-nanotube-filled latex.* Macromolecular Materials and Engineering, 2006. **291**(9): p. 1035-1043.
7. Yu, C., et al., *Thermoelectric behavior of segregated-network polymer nanocomposites.* Nano Letters, 2008. **8**(12): p. 4428-4432.
8. Vaisman, L., H.D. Wagner, and G. Marom, *The role of surfactants in dispersion of carbon nanotubes.* Advances in Colloid and Interface Science, 2006. **128**: p. 37-46.
9. Bandyopadhyaya, R., et al., *Stabilization of individual carbon nanotubes in aqueous solutions.* Nano Letters, 2002. **2**(1): p. 25-28.

10. Kymakis, E. and G.A.J. Amaratunga, *Electrical properties of single-wall carbon nanotube-polymer composite films.* Journal of Applied Physics, 2006. **99**(8): p. 084302:1-7.

11. Hermant, M.C., et al., *Lowering the percolation threshold of single-walled carbon nanotubes using polystyrene/poly(3,4-ethylenedioxythiophene): poly(styrene sulfonate) blends.* Soft Matter, 2009. **5**(4): p. 878-885.

12. Tummala, N.R. and A. Striolo, *SDS surfactants on carbon nanotubes: Aggregate morphology.* Acs Nano, 2009. **3**(3): p. 595-602.

13. Grossiord, N., et al., *Toolbox for dispersing carbon nanotubes into polymers to get conductive nanocomposites.* Chemistry of Materials, 2006. **18**(5): p. 1089-1099.

14. Wang, H., et al., *Dispersing single-walled carbon nanotubes with surfactants: A small angle neutron scattering study.* Nano Letters, 2004. **4**(9): p. 1789-1793.

15. Moore, V.C., et al., *Individually suspended single-walled carbon nanotubes in various surfactants.* Nano Letters, 2003. **3**(10): p. 1379-1382.

16. Grunlan, J.C., L. Liu, and O. Regev, *Weak polyelectrolyte control of carbon nanotube dispersion in water.* Journal of Colloid and Interface Science, 2008. **317**(1): p. 346-349.

17. Dror, Y., W. Pyckhout-Hintzen, and Y. Cohen, *Conformation of polymers dispersing single-walled carbon nanotubes in water: A small-angle neutron scattering study.* Macromolecules, 2005. **38**(18): p. 7828-7836.

18. Ouyang, B.Y., et al., *High-conductivity poly (3,4-ethylenedioxythiophene): poly(styrene sulfonate) film and its application in polymer optoelectronic devices.* Advanced Functional Materials, 2005. **15**(2): p. 203-208.

19. Ouyang, J., et al., *On the mechanism of conductivity enhancement in poly (3,4-ethylenedioxythiophene): poly(styrene sulfonate) film through solvent treatment.* Polymer, 2004. **45**(25): p. 8443-8450.

20. Haggenmueller, R., et al., *Comparison of the quality of aqueous dispersions of single wall carbon nanotubes using surfactants and biomolecules.* Langmuir, 2008. **24**(9): p. 5070-5078.

21. Zheng, M., et al., *DNA-assisted dispersion and separation of carbon nanotubes.* Nature Materials, 2003. **2**(5): p. 338-342.

22. Tsai, Y.C., et al., *Dispersion of carbon nanotubes in low pH aqueous solutions by means of alumina-coated silica nanoparticles.* Carbon, 2007. **45**(14): p. 2823-2827.

23. Liu, L. and J.C. Grunlan, *Clay assisted dispersion of carbon nanotubes in conductive epoxy nanocomposites.* Advanced Functional Materials, 2007. **17**(14): p. 2343-2348.

24. Kim, J.Y., et al., *Enhancement of electrical conductivity of poly(3,4-ethylenedioxythiophene)/poly(4-styrenesulfonate) by a change of solvents.* Synthetic Metals, 2002. **126**(2-3): p. 311-316.

25. Jagur-Grodzinski, J., *Electronically conductive polymers.* Polymers for Advanced Technologies, 2002. **13**(9): p. 615-625.

26. Kirchmeyer, S. and K. Reuter, *Scientific importance, properties and growing applications of poly(3,4-ethylenedioxythiophene).* Journal of Materials Chemistry, 2005. **15**(21): p. 2077-2088.

27. De, S., et al., *Transparent, Flexible, and Highly Conductive Thin Films Based on Polymer - Nanotube Composites.* Acs Nano, 2009. **3**(3): p. 714-720.

28. Ebbesen, T.W., et al., *Electrical conductivity of individual carbon nanotubes.* Nature, 1996. **382**(6586): p. 54-56.

29. Yu, C.H., et al., *Thermal conductance and thermopower of an individual single-wall carbon nanotube.* Nano Letters, 2005. **5**(9): p. 1842-1846.

30. Pop, E., et al., *Thermal conductance of an individual single-wall carbon nanotube above room temperature.* Nano Letters, 2006. **6**(1): p. 96-100.

31. Hone, J., et al., *Thermal properties of carbon nanotubes and nanotube-based materials.* Applied Physics a-Materials Science & Processing, 2002. **74**(3): p. 339-343.

32. Prasher, R.S., et al., *Turning carbon nanotubes from exceptional heat conductors into insulators.* Physical Review Letters, 2009. **102**(10): p. 105901:1-4.

33. Scholdt, M., et al., *Organic Semiconductors for Thermoelectric Applications.* Journal of Electronic Materials, 2010. **39**(9): p. 1589-1592.

34. Tans, S.J., A.R.M. Verschueren, and C. Dekker, *Room-temperature transistor based on a single carbon nanotube.* Nature, 1998. **393**(6680): p. 49-52.

35. Derycke, V., et al., *Carbon nanotube inter- and intramolecular logic gates.* Nano Lett., 2001. **1**(9): p. 453-456.

36. Liu, X.M., et al., *Transparent boron-doped carbon nanotube films.* Nano Letters, 2008. **8**(9): p. 2613-2619.

37. Hellstrom, S.L., H.W. Lee, and Z.N. Bao, *Polymer-assisted direct deposition of uniform carbon nanotube bundle networks for high performance transparent electrodes.* ACS Nano, 2009. **3**(6): p. 1423-1430.

38. Li, J., et al., *Highly-ordered carbon nanotube arrays for electronics applications.* Applied Physics Letters, 1999. **75**(3): p. 367-369.

39. Lee, N.S., et al., *Application of carbon nanotubes to field emission displays.* Diamond and Related Materials, 2001. **10**(2): p. 265-270.

40. Kymakis, E., I. Alexandrou, and G.A.J. Amaratunga, *High open-circuit voltage photovoltaic devices from carbon-nanotube-polymer composites.* Journal of Applied Physics, 2003. **93**(3): p. 1764-1768.

41. Kongkanand, A., R.M. Dominguez, and P.V. Kamat, *Single wall carbon nanotube scaffolds for photoelectrochemical solar cells. Capture and transport of photogenerated electrons.* Nano Letters, 2007. **7**(3): p. 676-680.

42. Ryu, Y. and C. Yu, *The influence of incorporating organic molecules or inorganic nanoparticles on the optical and electrical properties of carbon nanotube films.* Solid State Communications, 2011. **151**(24): p. 1932-1935.

43. Meng, C.Z., C.H. Liu, and S.S. Fan, *A promising approach to enhanced thermoelectric properties using carbon nanotube networks.* Adv. Mater., 2010. **22**(4): p. 535-539.

44. Yao, Q., et al., *Enhanced thermoelectric performance of single-walled carbon nanotubes/polyaniline hybrid nanocomposites.* Acs Nano, 2010. **4**(4): p. 2445-2451.

45. Kim, D., et al., *Improved thermoelectric behavior of nanotube-filled polymer composites with poly(3,4-ethylenedioxythiophene) poly(styrenesulfonate).* Acs Nano, 2010. **4**(1): p. 513-523.

46. Yu, C., et al., *Light-weight flexible carbon nanotube based organic composites with large thermoelectric power factors.* Acs Nano, 2011. **5**(10): p. 7885-7892.

47. Yu, C., et al., *Modulating electronic transport properties of carbon nanotubes to improve the thermoelectric power factor via nanoparticle decoration.* Acs Nano, 2011. **5**(2): p. 1297-1303.

48. Kaminishi, D., et al., *Air-stable n-type carbon nanotube field-effect transistors with Si3N4 passivation films fabricated by catalytic chemical vapor deposition.* Applied Physics Letters, 2005. **86**(11).

49. Kim, S.M., et al., *Reduction-controlled viologen in bisolvent as an environmentally stable n-type dopant for carbon nanotubes.* Journal of the American Chemical Society, 2009. **131**(1): p. 327-331.

50. Zhang, Z.Y., et al., *Doping-free fabrication of carbon nanotube based ballistic CMOS devices and circuits.* Nano Letters, 2007. **7**(12): p. 3603-3607.

51. Shim, M., et al., *Polymer functionalization for air-stable n-type carbon nanotube field-effect transistors.* Journal of the American Chemical Society, 2001. **123**(46): p. 11512-11513.

52. Ryu, Y.T., D. Freeman, and C.G. Yu, *High electrical conductivity and n-type thermopower from double-/single-wall carbon nanotubes by manipulating charge interactions between nanotubes and organic/inorganic nanomaterials.* Carbon, 2011. **49**(14): p. 4745-4751.

53. Yamaguchi, I. and T. Yamamoto, *Soluble self-doped single-walled carbon nanotube.* Materials Letters, 2004. **58**(5): p. 598-603.

54. Li, Z.R., et al., *Polymer functionalized n-type single wall carbon nanotube photovoltaic devices.* Applied Physics Letters, 2010. **96**(3).

55. Lin, Y.M., et al., *High-performance carbon nanotube field-effect transistor with tunable Polarities.* Ieee Transactions on Nanotechnology, 2005. **4**(5): p. 481-489.

56. Zebarjadi, M., et al., *Perspectives on thermoelectrics: from fundamentals to device applications.* Energy & Environmental Science, 2012. **5**(1): p. 5147-5162.

57. Snyder, G.J., *Application of the compatibility factor to the design of segmented and cascaded thermoelectric generators.* Applied Physics Letters, 2004. **84**(13): p. 2436-2438.

58. Das, N.C., et al., *Single-Walled Carbon Nanotube/Poly(methyl methacrylate) Composites for Electromagnetic Interference Shielding.* Polymer Engineering and Science, 2009. **49**(8): p. 1627-1634.

59. Zhu, D., Y.Z. Bin, and M. Matsuo, *Electrical conducting behaviors in polymeric composites with carbonaceous fillers.* Journal of Polymer Science Part B-Polymer Physics, 2007. **45**(9): p. 1037-1044.

60. Tritt, T.M., H. Boettner, and L. Chen, *Thermoelectrics: Direct Solar Thermal Energy Conversion.* Mrs Bulletin, 2008. **33**(4): p. 366-368.

61. Snyder, G.J. and E.S. Toberer, *Complex thermoelectric materials.* Nature Mater., 2008. **7**: p. 105.

62. Majumdar, A., *Thermoelectricity in Semiconductor Nanostructures.* Science, 2004. **303**: p. 777-778.

63. Winder, E.J., A.B. Ellis, and G.C. Lisensky, *Thermoelectric Devices: Solid-State Refrigerators and Electrical Generators in the Classroom.* J. Chem. Edu., 1996. **73**(10): p. 940-946.

64. Jackson, R.K., et al., *eEvaluation of transparent carbon nanotube networks of homogeneous electronic type.* Acs Nano, 2010. **4**(3): p. 1377-1384.

65. Blackburn, J.L., et al., *Transparent conductive single-walled carbon nanotube networks with precisely tunable ratios of semiconducting and metallic nanotubes.* Acs Nano, 2008. **2**(6): p. 1266-1274.

66. Collins, P.G., et al., *Extreme oxygen sensitivity of electronic properties of carbon nanotubes.* Science, 2000. **287**(5459): p. 1801-1804.

67. Jiang, F.X., et al., *Thermoelectric performance of poly(3,4-ethylenedioxythiophene): Poly(styrenesulfonate).* Chinese Physics Letters, 2008. **25**(6): p. 2202-2205.

68. Volkov, A.N. and L.V. Zhigilei, *Scaling Laws and Mesoscopic Modeling of Thermal Conductivity in Carbon Nanotube Materials.* Physical Review Letters, 2010. **104**(21).

69. Kim, W.J., et al., *Covalent functionalization of single-walled carbon nanotubes alters their densities allowing electronic and other types of separation.* Journal of Physical Chemistry C, 2008. **112**(19): p. 7326-7331.

70. Chalopin, Y., S. Volz, and N. Mingo, *Upper bound to the thermal conductivity of carbon nanotube pellets.* Journal of Applied Physics, 2009. **105**(8).

71. Unidym, *Product description: HiPco single wall carbon nanotubes.* http://www.unidym.com/files/Unidym_Product_Sheet_SWNT021810RevB.pdf, 2013.

72. CheapTubes, *Product information.* http://www.cheaptubesinc.com/swnts.htm, 2013.

73. CheapTubes, *Product information.* http://www.cheaptubesinc.com/MWNTs.htm, 2013.

74. Hu, X.J., L.N. Jiang, and K.E. Goodson, *Thermal conductance enhancement of particle-filled thermal interface materials using carbon nanotube inclusions.* Itherm, 2004. **1**(1): p. 63-69.

75. Wikipedia, *Gold.* http://en.wikipedia.org/wiki/Gold, 2013.

76. Collins, P.G. and P. Avouris, *Nanotubes for electronics.* Sci. Am., 2000. **283**(6): p. 62-69.

77. Park, W., et al., *Influence of nanomaterials in polymer composites on thermal conductivity.* J. Heat Trans.-T ASME, 2012. **134**(4): p. 041302.

78. Hugh W. Coleman, W.G.S., *Experimentation and uncertainty analysis for engineers* 2nd ed. 1999: Wiley-Interscience.

79. Choi, K. and C. Yu, *Highly doped carbon nanotubes with gold nanoparticles and their influence on electrical conductivity and thermopower of nanocomposites.* Plos One, 2012. **7**(9).

80. Forster, R.J. and L. Keane, *Nanoparticle-metallopolymer assemblies: charge percolation and redox properties.* J. Electroanal. Chem., 2003. **554**(1): p. 345-354.

81. Devadoss, A., et al., *Electrochemiluminescent Metallopolymer-Nanoparticle Composites: Nanoparticle Size Effects.* Analytical Chemistry, 2011. **83**(6): p. 2383-2387.

82. Podhajecka, K., O. Dammer, and J. Pfleger, *Electrical conductivity of poly(3-octylthiophene)/Au nanocomposites.* Macromol. Symp., 2008. **268**(1): p. 72-76.

83. Choi, H.C., et al., *Spontaneous reduction of metal ions on the sidewalls of carbon nanotubes.* Journal of the American Chemical Society, 2002. **124**(31): p. 9058-9059.

84. Kong, B.S., J.X. Geng, and H.T. Jung, *Layer-by-layer assembly of graphene and gold nanoparticles by vacuum filtration and spontaneous reduction of gold ions.* Chemical Communications, 2009(16): p. 2174-2176.

85. Wikipedia, *Standard electrode potential (data page).* http://en.wikipedia.org/wiki/Standard_electrode_potential_(data_page), 2013.

86. Kong, B.S., et al., *Single-walled carbon nanotube gold nanohybrids: Application in highly effective transparent and conductive films.* J. Phys. Chem. C, 2007. **111**(23): p. 8377-8382.

87. Yang, S.B., et al., *Effect of Au doping and defects on the conductivity of single-walled carbon nanotube transparent conducting network films.* Journal of Physical Chemistry C, 2010. **114**(20): p. 9296-9300.

88. Shiraishi, M. and M. Ata, *Work function of carbon nanotubes.* Carbon, 2001. **39**(12): p. 1913-1917.

89. Sun, J.P., et al., *Work function of single-walled carbon nanotubes determined by field emission microscopy.* Appl. Phys. A-Mater. Sci. Process., 2002. **75**(4): p. 479-483.

90. Ago, H., et al., *Work functions and surface functional groups of multiwall carbon nanotubes.* Journal of Physical Chemistry B, 1999. **103**(38): p. 8116-8121.

91. Riviere, J.C., *The work function of gold.* Appl. Phys. Lett., 1966. **8**(7): p. 172-173.

92. Sachtler, W.M., G.J.H. Dorgelo, and A.A. Holscher, *The work function of gold.* Surf. Sci., 1966. **5**(2): p. 221-229.

93. Ryu, Y., L. Yin, and C. Yu, *Dramatic electrical conductivity improvement of carbon nanotube networks by de-bundling and hole-doping with chlorosulfonic acid.* J. Mater. Chem., 2012. **22**: p. 6959-6964.

94. Rowe, D.M., *CRC Handbook of Thermoelectrics*. 1995, Boca Raton, Florida: CRC Press.

95. Ryu, Y., D. Freeman, and C. Yu, *High electrical conductivity and n-type thermopower from double-/single-wall carbon nanotubes by manipulating*

charge interactions between nanotubes and organic/inorganic nanomaterials. Carbon, 2011. **49**(14): p. 4745-4751.

96. Carroll, D.L., R. Czerw, and S. Webster, *Polymer-nanotube composites for transparent, conducting thin films.* Synthetic Metals, 2005. **155**(3): p. 694-697.

97. Zhang, B., et al., *Promising thermoelectric properties of commercial PEDOT:PSS materials and their Bi(2)Te(3) powder composites.* ACS Appl. Mater. Interfaces, 2010. **2**(11): p. 3170-3178.

98. Reyes-Reyes, M., I. Cruz-Cruz, and R. Lopez-Sandoval, *Enhancement of the electrical conductivity in PEDOT:PSS films by the addition of dimethyl sulfate.* Journal of Physical Chemistry C, 2010. **114**(47): p. 20220-20224.

99. Kim, J.Y., et al., *Enhancement of electrical conductivity of poly(3,4-ethylenedioxythiophene)/poly(4-styrenesulfonate) by a change of solvents.* Synth. Met., 2002. **126**(2): p. 311-316.

100. Hecht, D.S., et al., *High conductivity transparent carbon nanotube films deposited from superacid.* Nanotechnology, 2011. **22**(7): p. 075201-5.

101. Geng, H.Z., et al., *Dependence of material quality on performance of flexible transparent conducting films with single-walled carbon nanotubes.* Nano, 2007. **2**(3): p. 157-167.

102. Dai, H.J., E.W. Wong, and C.M. Lieber, *Probing electrical transport in nanomaterials: Conductivity of individual carbon nanotubes.* Science, 1996. **272**(5261): p. 523-526.

103. Freeman, D.D., K. Choi, and C. Yu, *N-type thermoelectric performance of functionalized carbon nanotube-filled polymer composites.* Plos One, 2012. **7**(11).

104. Ryu, Y., L. Yin, and C.H. Yu, *Dramatic electrical conductivity improvement of carbon nanotube networks by simultaneous de-bundling and hole-doping with chlorosulfonic acid.* Journal of Materials Chemistry, 2012. **22**(14): p. 6959-6964.

105. Dillon, E.P., C.A. Crouse, and A.R. Barron, *Synthesis, characterization, and carbon dioxide adsorption of covalently attached polyethyleneimine-functionalized single-wall carbon nanotubes.* Acs Nano, 2008. **2**(1): p. 156-164.

106. Liao, K.S., et al., *Optical limiting study of double wall carbon nanotube-Fullerene hybrids.* Chemical Physics Letters, 2010. **489**(4-6): p. 207-211.

107. Bubnova, O., et al., *Optimization of the thermoelectric figure of merit in the conducting polymer poly(3,4-ethylenedioxythiophene).* Nature Materials, 2011. **10**(6): p. 429-433.